

Shear viscosity and electrical conductivity of relativistic fluid in presence of magnetic field: a massless case

Jayanta Dey¹, Sarthak Satapathy¹, Prasanta Murmu^{2,1}, and Sabyasachi Ghosh¹

¹ Indian Institute of Technology Bhilai, GEC Campus, Sejbahar, Raipur 492015, Chhattisgarh, India

² Indian School of Mines Dhanbad 826004, Jharkhand, India.

Received: date / Revised version: date

Abstract. We have explored the shear viscosity and electrical conductivity calculations for bosonic and fermionic medium, which goes from without to with magnetic field picture and then their simplified massless expressions. In presence of magnetic field, 5 independent velocity gradient tensors can be designed, so their corresponding proportional coefficients, connected with the viscous stress tensor provide us 5 shear viscosity coefficients. In existing literature, two sets of tensors are available. Starting from them, present work has obtained two sets of expressions for 5 shear viscosity coefficients, which can be ultimately classified into three basic components - parallel, perpendicular and Hall components as one get same for electrical conductivity at finite magnetic field. Our calculations are based on kinetic theory approach in relaxation time approximation. Repeating same mathematical steps for finite magnetic field picture, which traditionally practiced for without field case, we have obtained 2 sets of 5 shear viscosity components, whose final expressions are in well agreements with earlier references, although a difference in methodology or steps can be clearly noticed. Realizing the massless results of viscosity and conductivity for Maxwell-Boltzmann, Fermi-Dirac and Bose-Einstein distribution function, we have applied them for massless quark gluon plasma and hadronic matter phases, which can provide us a rough order of strength, within which actual results will vary during quark-hadron phase transition. Present work also indicates that magnetic field might have some role for building perfect fluid nature in RHIC or LHC matter. The lower bound expectation of shear viscosity to entropy density ratio is also discussed.

PACS. XX.XX.XX No PACS code given

1 Introduction

Heavy-ion collisions have been the subject of intensive research to extract information about the nuclear properties of matter in extreme conditions like high temperature and high external magnetic fields. This field covers many interesting phenomena such as magnetic catalysis [1], chiral magnetic effect [2][3], inverse magnetic catalysis [4,5,6] etc. A detail discussion on the effects of magnetic field in quantum field theory has been addressed in Ref. [7]. A verification of these anticipated results is possible by studying QCD matter under the influence of electromagnetic fields. A review of the phase structure of QCD in the presence of magnetic field has been given in Ref. [8].

Ref. [9] shows analytically that fields produced in RHIC and LHC can reach up to m_π^2 and $10m_\pi^2$ respectively after collision. Possible space time evolution of electromagnetic fields, generated in heavy-ion collisions are well discussed in Refs. [10,11,12]. Applying that space time evolution of magnetic field information to the hydrodynamical expansion of quark-gluon plasma will construct a detail expansion dynamics, which is commonly known as magneto hydrodynamic (MHD). Under the influence of a strong

magnetic field the properties of quark-gluon plasma in heavy-ion collisions have been studied under the generalized framework of Bjorken flow [13,14]. In the limit of ideal magnetohydrodynamics, i.e., for infinite conductivity, and irrespective of the strength of the initial magnetization, the decay of the fluid energy density with proper time is the same as for the “Bjorken flow” without magnetic field. It has been found in Ref. [14] that under the influence of magnetic field the energy density and temperature decay slowly because of magnetic field. But taking into consideration the magnetic field produced in heavy-ion collisions the decay is suppressed. Numerical approaches to magnetohydrodynamics and its application to heavy-ion collisions have been studied [15,16]. Impact of external magnetic field through transport simulation can be noticed in Ref. [17]. For dissipative picture of MHD or transport simulation, field dependent transport coefficients might be required as inputs and therefore, a parallel microscopic calculation of transport coefficients in presence of magnetic field [18] is an important topic in heavy ion Physics community. In recent time transport coefficients in presence of magnetic field are investigated in Refs. [19,20,21,22,23,24,25,26,27,28,29,30,31,32,33,34,35,36,37,38,39,

40, 41, 42, 43, 44, 45, 46, 47, 48, 49, 50], where shear viscosity [19, 20, 21, 22, 23, 24, 25, 26, 27, 28, 29], electrical conductivity [30, 31, 32, 33, 34, 35, 36, 37, 38, 39, 40, 41, 42, 43], bulk viscosity [44, 45, 46, 47, 48] for light quark sector as well as field impact in heavy quark sector [49, 50] are studied. Transport coefficients at finite magnetic field in the direction of gauge gravity duality is also studied in Refs. [51, 52, 53].

In absence of magnetic field, any transport coefficient in different direction remain same i.e. an isotropic value is expected but in presence of magnetic field, a multi-component structure of the transport coefficient can be built, for which an anisotropic transportation in the fluid is expected. Among the earlier references, which have not considered the rich multi-component structure of transport coefficients, will not be our matter of interest. They may be considered for rough estimations of magnetic field dependent transport coefficients, but they have missed the vital anisotropic part of transport properties in presence magnetic field. So for getting complete picture, we should focus only those particular references, who have considered the multi-component structure in well manner. Reviewing all those references, who considered the multi-component structure of transport coefficients, present article intended to provide a complete and enriched understanding on those multi-component transport coefficients, mainly shear viscosity along with electrical conductivity.

Now, if we analyze the existing microscopic calculations of shear viscosity in presence of magnetic field [19, 21, 22, 25, 26, 27, 28, 29, 51, 52], then we can classify them into two groups. One group [19, 21, 22, 25, 26, 27] has considered a set of tensor structures, proposed by Ref. [18] and other group [28, 29, 51, 52] has considered another set of tensor structures, proposed by Ref. [61, 62]. Therefore, we find two sets of shear viscosities, which are also mutually inter-connected and can be linked with basic components like parallel, perpendicular and Hall components. Present article has attempted to provide the complete pictures of two set of shear viscosity components with their detail derivation in relaxation time approximation of kinetic theory approach. Although earlier Refs. [19, 21, 22, 26, 28] also addressed same final (simplified massless) expressions, but derivation of present work has its own uniqueness in its mathematical steps and approaches. After providing the complete picture two set of shear viscosity components with their general and then massless expressions, present work is also aimed to provide estimation first for three different distribution functions Maxwell-Boltzmann (MB), Fermi-Dirac (FD) and Bose-Einstein (BE), then for massless quark gluon plasma (QGP) and hadronic matter (HM) phases to visualize rough order of magnitude in two phases. At the end, lower bound aspects of shear viscosity to entropy density ratio is discussed.

The article is organized as follows. Sec. (2) covers a detail derivation of two sets of shear viscosity components at finite magnetic field along with brief description of electrical conductivity. Next in Sec. 3, we have explored the massless case results, where analytic expressions of different thermodynamical quantities and transport coefficients are obtained. Then in Sec. (4), we have explored the phe-

nomenological band of viscosity to entropy density ratio for quark gluon plasma without and with magnetic field pictures. In Sec. (5), the lower bound expectation of viscosity to entropy density ratio is discussed. At the end, Sec. (6) has summarized the investigations and few calculation gap are addressed in Sec. (8).

We use the natural unit with $\hbar = k = c = 1$ and metric tensor $g^{\mu\nu} = \text{diag}(+1, -1, -1, -1)$.

2 Expressions of transport coefficients in presence of magnetic field

2.1 Shear viscosity components using tensors of Ref. [18]

Before going to detail calculation of shear viscosity in presence of magnetic field, let us take a quick revisit of its without field expression. There are two approaches - Kubo framework [54, 55, 56] and kinetic theory framework [57, 58], which are popularly practiced for microscopic calculations of transport coefficients. Here we will follow the latter approach in relaxation time approximation (RTA).

Considering ideal ($T_0^{\mu\nu}$) and dissipative ($\Delta T^{\mu\nu}$) parts of energy-momentum tensor as a macroscopic outcomes of two microscopic quantities - equilibrium distribution function f_0 and its deviation δf (i.e. total distribution function $f = f_0 + \delta f$), one can express macroscopic and microscopic definition of dissipative energy momentum tensor (shear viscosity part only) as

$$\begin{aligned} \Delta T^{\mu\nu} &= \eta C^{\mu\nu} \text{ (Macro) ,} \\ \text{with } C^{\mu\nu} &= \left(\Delta^{\mu\alpha} \partial_\alpha u^\nu + \Delta^{\nu\alpha} \partial_\alpha u^\mu - \frac{2}{3} \Delta^{\mu\nu} \partial_\sigma u^\sigma \right) , \\ \Delta T^{\mu\nu} &= g \int \frac{d^3 \mathbf{k}}{(2\pi)^3} \frac{k^\mu k^\nu}{\omega} \delta f \text{ (Micro) ,} \end{aligned} \quad (1)$$

where η is shear viscosity coefficient, $\Delta^{\mu\nu} = g^{\mu\nu} - u^\mu u^\nu$, is the projection orthogonal to fluid velocity u^μ , $g^{\mu\nu}$ is the metric tensor, $\omega = \sqrt{\mathbf{k}^2 + m^2}$ is the energy of fluid particle with mass m and g is its degeneracy factor. Assuming $\delta f = C \frac{k_\sigma}{\omega} \frac{k_\rho}{\omega} C^{\sigma\rho}$ in terms of an unknown constant C , Eq. (1) will provide the expression of η :

$$\eta = \frac{2}{15} \int \frac{d^3 \mathbf{k}}{(2\pi)^3} C \frac{\mathbf{k}^4}{\omega^3} , \quad (2)$$

where the 1/15 factor comes after using the identity (in 3-vector notation):

$$\langle k^i k^j k^k k^l \rangle = \frac{1}{15} k^4 (\delta^{ij} \delta^{kl} + \delta^{il} \delta^{jk} + \delta^{ik} \delta^{jl}) . \quad (3)$$

With the help of the RTA in relativistic Boltzmann equation (RBE), the values of unknown constant can be obtained as $C = -\frac{\beta \tau_c \omega}{2} f_0 (1 - a f_0)$ [57, 58], where distribution function $f_0 = 1/\{e^{\beta\omega} + a\}$ will be Fermi-Dirac (FD), Bose-Einstein (BE) and Maxwell-Boltzmann (MB)

for $a = +1, -1, 0$. Hence, Eq. (2) will get the final form [57, 58],

$$\eta = \frac{g\beta}{15} \int \frac{d^3\mathbf{k}}{(2\pi)^3} \frac{\mathbf{k}^4}{\omega^2} \tau_c f_0 (1 - af_0). \quad (4)$$

Following the similar steps, adopted earlier for $B = 0$ case [57, 58], we will now proceed for calculation of shear viscosity in presence of a magnetic field. As viscosity is nothing to do with the time component, so, we can do the calculation by dropping the time component also. For simplicity, in rest of the calculation we use 3-vector and instead of Greek letters used for 4-vector in the above calculations we use i, j, k, \dots for 3-vector.

In presence of a magnetic field (\mathbf{B}) we can find 5 independent traceless tensor components C_{ij}^n (n denotes different components which runs from 0 to 4) [18, 19] instead of a single tensor component C_{ij} . Hence, similar to Eq. (1), the macroscopic to microscopic connection will be [18, 19] (in 3-vector notation):

$$\begin{aligned} \Delta T_{ij} &= \sum_{n=0}^4 \eta_n C_{ij}^n \text{ (Macro)} \\ &= g \int \frac{d^3\mathbf{k}}{(2\pi)^3} v_i v_j \omega \delta f \text{ (Micro)} \end{aligned} \quad (5)$$

where $v_i \equiv \mathbf{k}/\omega$ ($= \mathbf{v}$) is particle velocity, η_n are 5 viscosity coefficients associated with 5 independent traceless tensors [18]:

$$\begin{aligned} C_{ij}^0 &= (3b_i b_j - \delta_{ij})(b_k b_l V_{kl} - (1/3)\nabla \cdot \mathbf{V}), \\ C_{ij}^1 &= 2V_{ij} + \delta_{ij} V_{kl} b_k b_l - 2V_{ik} b_k b_j - 2V_{jk} b_k b_i \\ &\quad (b_i b_j - \delta_{ij}) \nabla \cdot \mathbf{V} + b_i b_j V_{kl} b_k b_l, \\ C_{ij}^2 &= 2(V_{ik} b_j b_k + V_{jk} b_i b_k - 2b_i b_j V_{kl} b_k b_l), \\ C_{ij}^3 &= V_{ik} b_j b_k + V_{jk} b_i b_k - V_{kl} b_{ik} b_j b_l - V_{kl} b_{jk} b_i b_l, \\ C_{ij}^4 &= 2(V_{kl} b_{ik} b_j b_l + V_{kl} b_{jk} b_i b_l). \end{aligned} \quad (6)$$

Where, $V_{ij} = \frac{1}{2} \left(\frac{\partial V_i}{\partial x_j} + \frac{\partial V_j}{\partial x_i} \right)$ with fluid velocity $V_i \equiv \mathbf{V}$. $b_i \equiv \mathbf{B}/|B|$ is unit vector along the direction of magnetic field \mathbf{B} and $b_{ij} = \varepsilon_{ijk} b_k$, ε_{ijk} is total anti-symmetric Levi-Civita tensor. The reason of changes from single possible traceless tensor C^{ij} (at $B = 0$) to multiple independent traceless tensors C_{ij}^n (at $B \neq 0$) is as follows. The C^{ij} is built by V^i and δ^{ij} only, but C_{ij}^n has some additional building blocks b_i and b_{ij} .

Similar to $B = 0$ case, assuming δf in terms of unknown constant C_n (for $B = 0$ case, it was 1 unknown constant C , now for $B \neq 0$, it is 5 unknown constant C_n) [18, 19]:

$$\delta f = \sum_{n=0}^4 C_n C_{kl}^n v_k v_l, \quad (7)$$

Eq. (5) will give us expressions of η_n in terms of C_n :

$$\eta_n = -\frac{2}{15} \int \frac{d^3\mathbf{k}}{(2\pi)^3} \omega C_n \mathbf{v}^4. \quad (8)$$

With the help of RTA version of RBE, one can find the unknown constants C_n . Refs. [18, 19] have found these unknown constants in strong field limit. Present work has found its general expressions, valid for all ranges of magnetic field. Refs. [21, 26] have also found similar kind of general expressions, whose final expressions are exactly same as obtained in present draft, although reader can identify the differences in mathematical steps. Ref. [21] has explored the root of the traceless independent tensors C_{ij}^n from the simple possible form of independent tensors with building blocks δ_{ij} , b_i and b_{ij} . While Ref. [26] has gone through the similar mathematical structure via projection operator technique. In this context, present calculations show its quick and easy path for those reader, who are acquainted with the 5 possible independent traceless tensors C_{ij}^n . By repeating the similar steps of $B = 0$ case, prescribed in Refs. [58, 57] one can easily find the respective coefficients η_n , linked with C_{ij}^n . Present article has basically explored it.

Now, let us proceed to find C_n from RTA based RBE in presence of magnetic field, whose mathematical form looks like:

$$\begin{aligned} \frac{1}{\omega} p_i \frac{\partial f}{\partial x_i} + \frac{1}{\omega} q F_{ij} p_i \frac{\partial f}{\partial p_j} &= -\frac{\delta f}{\tau_c} \\ -\frac{\omega}{T} v_i v_j V_{ij} f_0 (1 - af_0) - \frac{qB}{\omega} b_{ij} v_j \frac{\partial}{\partial v_i} (\delta f) &= -\frac{\delta f}{\tau_c} \end{aligned} \quad (9)$$

where electromagnetic field-strength tensor $F_{ij} = -B b_{ij}$ is applied on q charge. Through this second term of left hand side (LHS), magnetic field enters into the calculation. LHS of RBE is considered $f \approx f_0$, where $\frac{\partial f_0}{\partial x_i}$ will give 1st term of lhs but 2nd term will be vanished. For getting non-zero values of 2nd term, which will basically consist of B-dependent term, we have to consider δf correction term. Hence 2nd term of lhs carry $\frac{\partial(\delta f)}{\partial v_j}$. Similar to relaxation time τ_c , we will get another time scale $\tau_B = \omega/(qB)$ in Eq. (9), which is similar to inverse of cyclotron frequency. Former is mainly controlled by randomness of the medium at particular temperature T , but it may also have dependence with magnetic field. Although in present work, we will consider it as free parameter. The τ_B is completely originated from external magnetic field and inversely depends on it.

Now by using δf from Eq. (7) in Eq. (9), we get

$$\begin{aligned} \frac{\omega}{T} v_i v_j V_{ij} f_0 (1 - af_0) &= -\frac{1}{\tau_B} b_{ij} v_j \frac{\partial}{\partial v_i} \left(\sum_{n=0}^4 C_n C_{kl}^n v_k v_l \right) \\ &\quad + \frac{1}{\tau_c} \left(\sum_{n=0}^4 C_n C_{kl}^n v_k v_l \right) \\ \Rightarrow \frac{\omega}{T} v_i v_j V_{ij} f_0 (1 - af_0) &= -\frac{1}{\tau_B} b_{ij} v_j 2 \times \left(\sum_{n=0}^4 C_n C_{ik}^n v_k \right) \\ &\quad + \frac{1}{\tau_c} \left(\sum_{n=0}^4 C_n C_{kl}^n v_k v_l \right) \end{aligned} \quad (10)$$

Now, comparing same tensor structure on both side (whose details calculations are given in Appendix, labeled as Sec. (7.1)) we get,

$$\begin{aligned} C_1 &= -\frac{\omega}{2T} \frac{\tau_c}{4 \left\{ \frac{1}{4} + (\tau_c/\tau_B)^2 \right\}} f_0(1 - af_0) \\ C_2 &= -\frac{\omega}{2T} \frac{\tau_c}{1 + (\tau_c/\tau_B)^2} f_0(1 - af_0) \\ C_3 &= -\frac{\omega}{2T} \frac{\tau_c \left(\frac{\tau_c}{\tau_B} \right)}{2 \left\{ \frac{1}{4} + (\tau_c/\tau_B)^2 \right\}} f_0(1 - af_0) \\ C_4 &= -\frac{\omega}{2T} \frac{\tau_c \left(\frac{\tau_c}{\tau_B} \right)}{1 + (\tau_c/\tau_B)^2} f_0(1 - af_0) \end{aligned} \quad (11)$$

Now, using expressions of C_s from eq. (11) in eq. (8) we get,

$$\begin{aligned} \eta_1 &= \frac{g\beta}{15} \int \frac{d^3\mathbf{k}}{(2\pi)^3} \left(\frac{\mathbf{k}^2}{\omega} \right)^2 \tau_c \frac{1}{4 \left\{ \frac{1}{4} + (\tau_c/\tau_B)^2 \right\}} \{f_0(1 - af_0)\} \\ \eta_2 &= \frac{g\beta}{15} \int \frac{d^3\mathbf{k}}{(2\pi)^3} \left(\frac{\mathbf{k}^2}{\omega} \right)^2 \tau_c \frac{1}{1 + (\tau_c/\tau_B)^2} \{f_0(1 - af_0)\} \\ \eta_3 &= \frac{g\beta}{15} \int \frac{d^3\mathbf{k}}{(2\pi)^3} \left(\frac{\mathbf{k}^2}{\omega} \right)^2 \tau_c \frac{\tau_c/\tau_B}{2 \left\{ \frac{1}{4} + (\tau_c/\tau_B)^2 \right\}} \{f_0(1 - af_0)\} \\ \eta_4 &= \frac{g\beta}{15} \int \frac{d^3\mathbf{k}}{(2\pi)^3} \left(\frac{\mathbf{k}^2}{\omega} \right)^2 \tau_c \frac{\tau_c/\tau_B}{1 + (\tau_c/\tau_B)^2} \{f_0(1 - af_0)\}. \end{aligned} \quad (12)$$

Now, one can find $C_{ij}^0 = 0$ for zero bulk viscosity case where $\nabla \cdot \mathbf{V} = V_{ii} = 0$, and $V_{ij}b_ib_j = 0$. However η_0 might have a non-zero value, which may not be obtained via earlier methodology, so we might have to find some alternative way. From eq. (6) we can find that C_{ij}^0 is parallel to magnetic field because $C_{ij}^0 b_ib_j \neq 0$. As in the field direction Lorentz force has no effect, so, η_0 should be same as in zero magnetic field ($B = 0$), which is given in eq. (4)

$$\eta_0 = \eta = \frac{g\beta}{15} \int \frac{d^3\mathbf{k}}{(2\pi)^3} \frac{\mathbf{k}^4}{\omega^2} \tau_c f_0(1 - af_0). \quad (13)$$

Our conclusion can be checked by alternative calculations, done in Refs. [21,26].

Limiting Cases: These four different viscosity components can be treated as more general expressions, which can be able to generate the expressions of strong field limit, addressed in Refs. [18,19] as a special case of them. Two possible limiting cases are discussed below.

For $B \rightarrow 0$, $\tau_B \rightarrow \infty$, we get

$$\begin{aligned} \eta_2 &= \eta_1 \\ &= \frac{g\beta}{15} \int \frac{d^3\mathbf{k}}{(2\pi)^3} \tau_c \left(\frac{\mathbf{k}^2}{\omega} \right)^2 [f_0\{1 - af_0\}] \\ &= \eta \end{aligned} \quad (14)$$

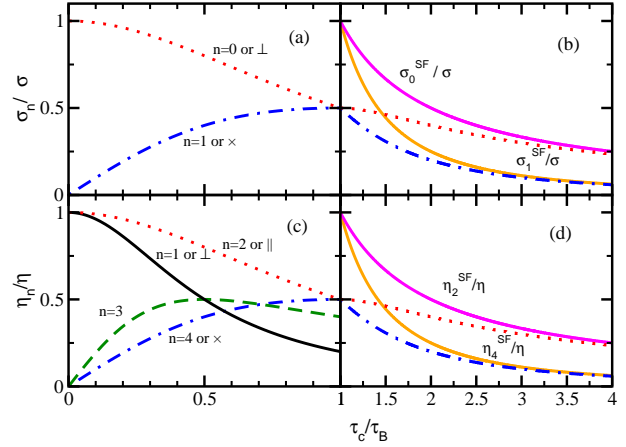


Fig. 1. Ratio of conductivity (a,b) and viscosity (c,d) with and without magnetic field along $\frac{\tau_c}{\tau_B}$ axis, which is classified into two: $\frac{\tau_c}{\tau_B} < 1$ (a,c) and $\frac{\tau_c}{\tau_B} > 1$ (b,d).

and

$$\eta_4 = \eta_3 = 0. \quad (15)$$

One can identify $\eta_{1,2}$ as normal shear viscosity as they merge to η at $B \rightarrow 0$. Seeing the vanishing values of $\eta_{3,4}$ in absence of magnetic field, one can realize them as Hall-type shear viscosity, as they completely originate from qB and odd function of qB . So, let us relate them with other notations like $\eta_{\parallel, \perp}$, used in earlier Refs. [51,52], based on holographic dual theory. If the magnetic field is applied along z direction, then η_{xyxy} and $\eta_{xzzz} = \eta_{yzyz}$ can be called as perpendicular and parallel components. We have identified the relations:

$$\begin{aligned} \eta_{xyxy} &= \eta_{\perp} = \eta_1 \\ \eta_{xzzz} &= \eta_{yzyz} = \eta_{\parallel} = \eta_2. \end{aligned} \quad (16)$$

Sometimes the Hall viscosity components $\eta_{3,4}$ is denoted as η_{\times} [26].

If we take strong field (SF) limit $B \rightarrow \infty$, for which $\tau_B \rightarrow 0$, then we will get

$$\begin{aligned} \eta_2 &= 4\eta_1 \\ &= \frac{g\beta}{15} \int \frac{d^3\mathbf{k}}{(2\pi)^3} \frac{\tau_B^2}{\tau_c} \left(\frac{\mathbf{k}^2}{\omega} \right)^2 [f_0\{1 - af_0\}] \\ &= \eta_2^{SF} \text{ (say)} \end{aligned} \quad (17)$$

and

$$\begin{aligned} \eta_4 &= 2\eta_3 \\ &= \frac{g\beta}{15} \int \frac{d^3\mathbf{k}}{(2\pi)^3} \tau_B \left(\frac{\mathbf{k}^2}{\omega} \right)^2 [f_0\{1 - af_0\}] \\ &= \eta_4^{SF} \text{ (say)}. \end{aligned} \quad (18)$$

Exactly same expressions have been obtained in Refs. [19,18] in terms of MB distribution, where the calculations are done in strong field assumption.

2.2 Shear viscosity components using tensors of Ref. [61, 62]

In this section, we will find other set of shear viscosity components η_n if we start with other set of independent traceless tensors (C_{ij}^n) instead previous set, given in Eq. (6). This other set of tensors is proposed in Refs. [61, 62] and their structures are given below:

$$\begin{aligned} C_{ij}^0 &= 2(V_{ij} + (1/3)\delta_{ij}\nabla \cdot \mathbf{V}) \\ C_{ij}^1 &= \frac{3}{4}\{(3b_i b_j - \delta_{ij})(b_k b_l V_{kl} - (1/3)\nabla \cdot \mathbf{V})\} \\ C_{ij}^2 &= 2(V_{ik} b_j b_k + V_{jk} b_i b_k - 2V_{ij} b_i b_j b_k b_l) \\ C_{ij}^3 &= 2(V_{ik} b_{jk} + V_{jk} b_{ik} - V_{kl} b_{jl} b_i b_k - V_{kl} b_{il} b_j b_k) \\ C_{ij}^4 &= 2(b_{ik} b_j b_l + b_{jk} b_i b_l) V_{kl} \end{aligned} \quad (19)$$

All notations have same meaning as in the previous section.

Now, using C_{ij} s of Eq. (19) in Eq. (10), one can find all C_n as done for earlier subsection. The details of C_n calculations are addressed in Appendix - Sec. (7.2). Using those C_n 's, we get the final expressions of η_n as,

$$\begin{aligned} \eta_0 &= \frac{g\beta}{15} \int \frac{d^3 \mathbf{k}}{(2\pi)^3} \left(\frac{\mathbf{k}^2}{\omega}\right)^2 \tau_c \frac{1}{\{1 + 4(\tau_c/\tau_B)^2\}} \\ &\quad \{f_0(1 - af_0)\}, \\ \eta_2 &= \frac{3g\beta}{15} \int \frac{d^3 \mathbf{k}}{(2\pi)^3} \left(\frac{\mathbf{k}^2}{\omega}\right)^2 \tau_c \frac{(\tau_c/\tau_B)^2}{\{1 + 4(\tau_c/\tau_B)^2\}\{1 + (\tau_c/\tau_B)^2\}} \\ &\quad \{f_0(1 - af_0)\}, \\ \eta_3 &= \frac{g\beta}{15} \int \frac{d^3 \mathbf{k}}{(2\pi)^3} \left(\frac{\mathbf{k}^2}{\omega}\right)^2 \tau_c \frac{(\tau_c/\tau_B)}{\{1 + 4(\tau_c/\tau_B)^2\}} \\ &\quad \{f_0(1 - af_0)\}, \\ \eta_4 &= \frac{g\beta}{15} \int \frac{d^3 \mathbf{k}}{(2\pi)^3} \left(\frac{\mathbf{k}^2}{\omega}\right)^2 \tau_c \frac{(\tau_c/\tau_B)}{\{1 + (\tau_c/\tau_B)^2\}} \\ &\quad \{f_0(1 - af_0)\}. \end{aligned} \quad (20)$$

Now, only η_1 can not be obtained from RBE, so we will find some alternative way to obtain its expression. We see that Among the earlier set of C_{ij}^n in Eq. (6), only C_{ij}^0 is parallel to magnetic field ($C_{ij}^0 b_i b_j \neq 0$). Similarly, for present set of C_{ij}^n in Eq. (19), C_{ij}^0 and C_{ij}^1 are components of shear-stress tensor parallel to magnetic field. However, we don't find the expressions of η_0 and η_1 are equal to η but if we take linear combination of η_0 and $\frac{3}{4}\eta_1$ and demand

$$\eta_0 + \frac{3}{4}\eta_1 = \eta, \quad (21)$$

then we can get

$$\eta_1 = \frac{16}{3} \frac{g\beta}{15} \int \frac{d^3 \mathbf{k}}{(2\pi)^3} \frac{\mathbf{k}^4}{\omega^2} \tau_c \frac{(\tau_c/\tau_B)^2}{\{1 + 4(\tau_c/\tau_B)^2\}} \quad (22)$$

$$f_0(1 - af_0), \quad (23)$$

which is exactly same (massless expressions), as obtained by Ref. [28]. In latter section, we will find that our massless expressions of η_n (obtained from RTA based kinetic theory) are exactly same as obtained by Ref. [28] (in RTA based methods of moment technique).

When we compare present set of coefficients with earlier coefficients, we can identify two categories - one category is already existed at $B = 0$ picture, while other category does not. It means that the coefficients of latter category are completely appeared due to magnetic field. Hence, they can be called as magnetically induced coefficients. To distinguish between two sets of coefficients, let us modify the notations of earlier coefficient of Sec. (2.1) as $\tilde{\eta}_{0,1,2,3,4}$ from here.

One can easily realize that similar to $\tilde{\eta}_{3,4}$, the $\eta_{1,2,3,4}$ are magnetically induced coefficients as all are disappeared at $B \rightarrow 0$ or $\tau_B \rightarrow \infty$. Among them $\tilde{\eta}_{3,4}$ and $\eta_{3,4}$ are Hall coefficients, which are odd function of τ_B or eB . They are connected as

$$\begin{aligned} \eta_3 &= \frac{\tilde{\eta}_3}{2} \\ \eta_4 &= \tilde{\eta}_4. \end{aligned} \quad (24)$$

One can now find similarities between η_0 and $\tilde{\eta}_{1,2}$ as these are not vanished at $B = 0$. They are connected as

$$\begin{aligned} \eta_0 &= \tilde{\eta}_1 \\ \eta_0 + \eta_2 &= \tilde{\eta}_2. \end{aligned} \quad (25)$$

Remembering the $\eta_{\parallel,\perp}$ components in Eq. (16), we can identify the relations:

$$\begin{aligned} \eta_{\perp} &= \eta_0 = \tilde{\eta}_1 \\ \eta_{\parallel} &= \eta_0 + \eta_2 = \tilde{\eta}_2. \end{aligned} \quad (26)$$

Remaining coefficients are connected as

$$\begin{aligned} \eta_2 &= \tilde{\eta}_2 - \tilde{\eta}_1 \\ \eta_0 + \frac{3}{4}\eta_1 &= \tilde{\eta}_0 = \eta. \end{aligned} \quad (27)$$

So instead of being confused with too many coefficients, we should be focus on the gross physics, which is as follows. In absence of magnetic field, shear viscosity in different direction remain same and this isotropic value is defined as η here. Now, in presence of magnetic field this isotropic property breaks and we get different values of η_{\parallel} and η_{\perp} , which will be merged to η at $B \rightarrow 0$ i.e.

$$\lim_{B \rightarrow 0} \eta_{\parallel} \rightarrow \eta \leftarrow \lim_{B \rightarrow 0} \eta_{\perp}. \quad (28)$$

In terms of two sets of coefficients, we can write as

$$\begin{aligned} \lim_{B \rightarrow 0} \tilde{\eta}_2 &\rightarrow \tilde{\eta}_0 \leftarrow \lim_{B \rightarrow 0} \tilde{\eta}_1, \\ \lim_{B \rightarrow 0} (\eta_0 + \eta_2) &\rightarrow \left(\eta_0 + \frac{3}{4}\eta_1\right) \leftarrow \lim_{B \rightarrow 0} \eta_0. \end{aligned} \quad (29)$$

There also be Hall viscosity η_{\times} , which is absent at $B \rightarrow 0$ and that can be mathematically represented as

$$\begin{aligned} \lim_{B \rightarrow 0} \eta_{\times} &\rightarrow 0 \\ \lim_{B \rightarrow 0} \tilde{\eta}_{3,4} &\rightarrow 0 \\ \lim_{B \rightarrow 0} \eta_{3,4} &\rightarrow 0. \end{aligned} \quad (30)$$

2.3 Electrical conductivity components

Next, we come to the expression of electrical conductivity in presence of the magnetic field. Here, again we can first recall without magnetic field expression of the electrical conductivity,

$$\sigma = e^2 g \beta \frac{1}{3} \int \frac{d^3 \mathbf{k}}{(2\pi)^3} \frac{\mathbf{k}^2}{\omega^2} \tau_c f_0 (1 - f_0), \quad (31)$$

where, e is elementary charge and all other symbols have same meaning as in the above subsections. Then, instead of repeating its formalism for $\mathbf{B} \neq 0$ case, given in Refs.[30], let us come directly to final expressions

$$\sigma_n = e^2 g \beta \frac{1}{3} \int \frac{d^3 \mathbf{k}}{(2\pi)^3} \frac{\mathbf{k}^2}{\omega^2} \frac{\tau_c (\tau_c / \tau_B)^n}{1 + (\tau_c / \tau_B)^2} f_0 (1 - f_0), \quad (32)$$

where, n can take any value from 0 to 2, and σ_0 is normal conductivity along xx or yy direction, σ_1 is Hall conductivity along xy or yx direction and $\sigma_{zz} = \sigma_0 + \sigma_2 = \sigma$ is longitudinal conductivity if B is applied along z -direction. Alternative notations $\sigma_{\perp} = \sigma_0$, $\sigma_{\parallel} = \sigma_0 + \sigma_2$ and $\sigma_{\times} = \sigma_1$ are also used in earlier references [26, 38, 39].

Here also, magnetic field create anisotropic conduction ($\sigma_{\perp} \neq \sigma_{\parallel}$) and a magnetically induced Hall conductivity σ_{\times} . At $B \rightarrow 0$, restoring the isotropic property and vanishing Hall conductivity can be mathematically expressed as

$$\begin{aligned} \lim_{B \rightarrow 0} \sigma_{\perp} &\rightarrow \sigma_{\parallel} = \sigma \\ \lim_{B \rightarrow 0} \sigma_{\times} &\rightarrow 0. \end{aligned} \quad (33)$$

In strong field limit $B \rightarrow \infty$, we will get:

$$\begin{aligned} \sigma_0 &= \frac{g \beta e^2}{3} \int \frac{d^3 \mathbf{k}}{(2\pi)^3} \frac{\tau_B^2}{\tau_c} \left(\frac{\mathbf{k}^2}{\omega} \right)^2 [f_0 \{1 - a f_0\}] \\ &= \sigma_0^{SF} \text{(say)} \end{aligned} \quad (34)$$

and

$$\begin{aligned} \sigma_1 &= \frac{g \beta e^2}{3} \int \frac{d^3 \mathbf{k}}{(2\pi)^3} \tau_B \left(\frac{\mathbf{k}^2}{\omega} \right)^2 [f_0 \{1 - a f_0\}] \\ &= \sigma_1^{SF} \text{(say)} \end{aligned} \quad (35)$$

Analytic outcomes of $\eta_{\parallel, \perp, \times}$ and $\sigma_{\parallel, \perp, \times}$ for two opposite limits are drawn in Fig. 1(a-d) for getting better visualization. $B \rightarrow 0$ and $B \rightarrow \infty$ can be alternatively realized by $\tau_c / \tau_B \rightarrow 0$ and $\tau_c / \tau_B \rightarrow \infty$ or $\tau_c / \tau_B \ll 1$ and $\tau_c / \tau_B \gg 1$ in numerical point of view. In Fig. 1(a) and (b), $\sigma_{\parallel, \perp, \times}$ and $\eta_{\parallel, \perp, \times}$ are plotted against τ_c / τ_B from 0 to 1, where we can find the merging σ_{\perp} to $\sigma_{\parallel} = \sigma$ and $\eta_{\parallel, \perp}$ to η at $\tau_c / \tau_B = 0$. It means that we can get back our isotropic values of conductivity (σ) and shear viscosity (η) in absence of magnetic field just by putting $B \rightarrow 0$ or $\tau_c / \tau_B \rightarrow 0$. On the other hand, Hall conductivity σ_{\times} and shear viscosity components η_{\times} is disappeared at $B \rightarrow 0$ or $\tau_c / \tau_B \rightarrow 0$ as it is completely magnetic field induced

phenomena. Next, in Fig. 1(c) and (d), $\sigma_{\perp, \times}$, $\eta_{\perp, \times}$ are extended for $\tau_c / \tau_B > 1$ with same line-style curves. By using approximation $\tau_c / \tau_B \gg 1$, we have already got strong field limit expressions of $\sigma_{\perp, \times}$, $\eta_{\perp, \times}$, which are renamed as $\sigma_{\perp, \times}^{SF}$ in Eqs. (34), (35) and $\eta_{\perp, \times}^{SF}$ in Eqs. (17), (18). Plotting them against τ_c / τ_B -axis, we notice that $\sigma_{\perp, \times}$, $\eta_{\perp, \times}$ are merging to $\sigma_{\perp, \times}^{SF}$, and $\eta_{\perp, \times}^{SF}$ around and beyond $\tau_c / \tau_B = 4$. It means that we can safely use strong field approximated expressions for $\tau_c / \tau_B \geq 4$ but they can not be used for $\tau_c / \tau_B < 4$.

3 For massless Bosonic and Fermionic matter

3.1 Thermodynamics for $B = 0$

Here, we will address the analytic forms of thermodynamical quantities like energy density ϵ , pressure P , entropy density s for different systems of massless particles following Maxwell-Boltzmann (MB), Bose-Einstein (BE) and Fermi-Dirac (FD) distribution. To estimate η/s in Sec. (4), s is our main required quantity here.

In terms of distribution function f_0 , the energy density and pressure of any medium can be expressed as

$$\begin{aligned} \epsilon &= g \int_0^{\infty} \frac{d^3 \mathbf{p}}{(2\pi)^3} \omega f_0, \\ P &= g \int_0^{\infty} \frac{d^3 \mathbf{p}}{(2\pi)^3} \frac{\mathbf{p}^2}{3\omega} f_0, \end{aligned} \quad (36)$$

which are connected as $P = \frac{1}{3}\epsilon$ for massless case. So, entropy density of the system is

$$\begin{aligned} s &= \frac{\epsilon + P}{T} = \frac{4\epsilon}{3T} \\ &= \frac{4g\beta}{3} \int_0^{\infty} \frac{d^3 \mathbf{p}}{(2\pi)^3} \omega f_0 \end{aligned} \quad (37)$$

Solving Eq. (37) with $\mathbf{p} = \omega$ as for massless case, we get (See Sec. (8.1) in Appendix)

$$\begin{aligned} s &= \frac{4g}{\pi^2} T^3 \text{ for MB} \\ &= \frac{4g}{\pi^2} \zeta(4) T^3 = \frac{4g\pi^2}{90} T^3 \text{ for BE} \\ &= \left(\frac{7}{8}\right) \frac{4g}{\pi^2} \zeta(4) T^3 = \frac{7g\pi^2}{180} T^3 \text{ for FD,} \end{aligned} \quad (38)$$

where

$$\begin{aligned} \zeta(4) &= \frac{1}{\Gamma(4)} \int_0^{\infty} \frac{x^3}{(e^x - 1)} \\ &= \sum_{n=1}^{\infty} \frac{1}{n^4} = \frac{\pi^4}{90}. \end{aligned} \quad (39)$$

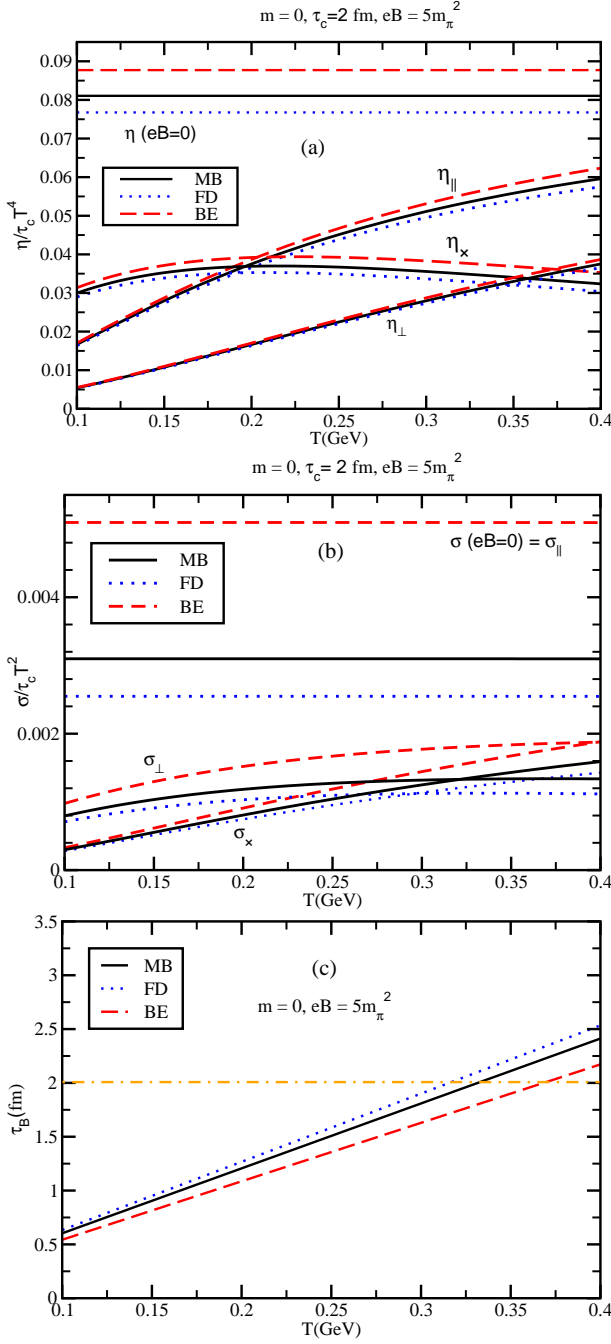


Fig. 2. $\eta/(\tau_c T^4)$, $\eta_{\parallel}/(\tau_c T^4)$, $\eta_{\perp}/(\tau_c T^4)$, $\eta_{\times}/(\tau_c T^4)$ vs T (upper panel) $\sigma/(\tau_c T^2)$, $\sigma_{\perp}/(\tau_c T^2)$, $\sigma_{\times}/(\tau_c T^2)$ vs T (middle panel) for MB, FD and BE distributions. Lower panel: magnetic time scale for MB, FD and BE distributions

3.2 Shear viscosity and electrical conductivity for $B = 0$

Now, let us come to shear viscosity and electrical conductivity expressions for massless and $B = 0$ case. By solving Eq. (4) for massless case, one can get (See Sec. (8.2) in Appendix):

$$\eta = \frac{4g}{5\pi^2} \tau_c T^4 \quad \text{for MB}$$

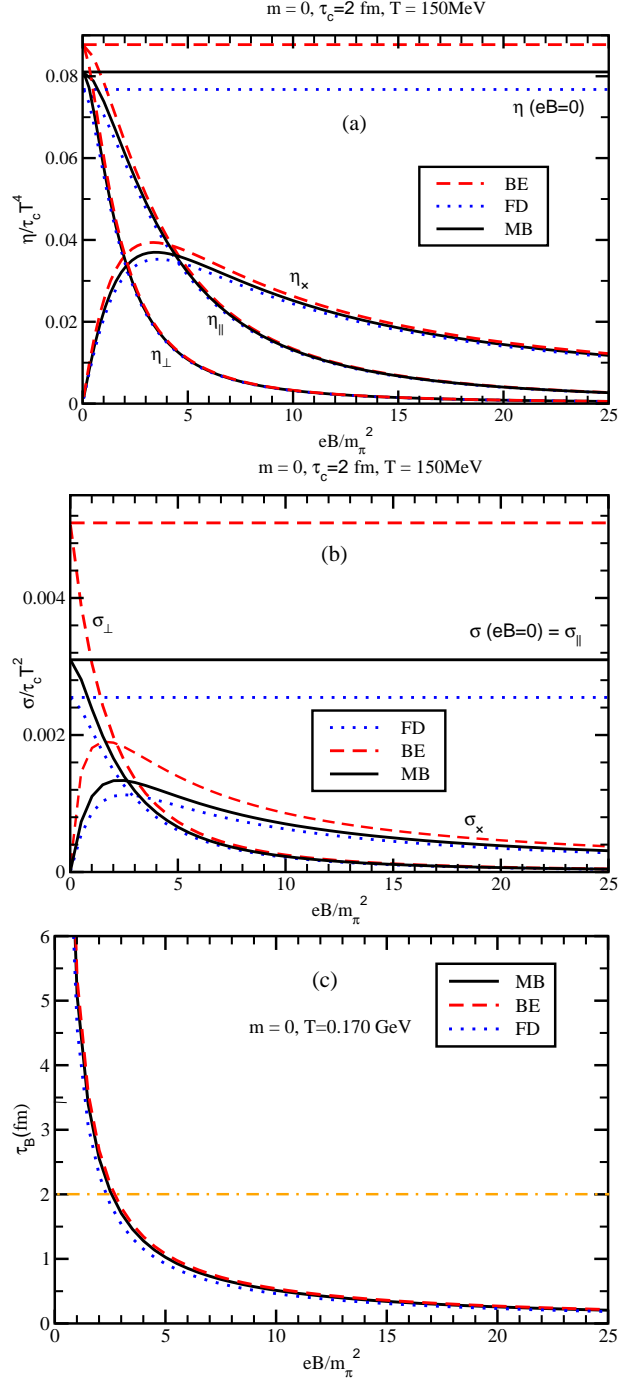


Fig. 3. Same as Fig. (2) along eB/m_{π}^2 -axis

$$\begin{aligned} &= \frac{4g}{5\pi^2} \tau_c \zeta(4) T^4 = \frac{4g\pi^2}{450} \tau_c T^4 \quad \text{for BE} \\ &= \left(\frac{7}{8}\right) \frac{4g}{5\pi^2} \tau_c \zeta(4) T^4 = \frac{7g\pi^2}{900} \tau_c T^4 \quad \text{for FD} \end{aligned} \quad (40)$$

and solving Eq. (31) for massless case, we get:

$$\begin{aligned} \sigma &= \frac{ge^2}{3\pi^2} \tau_c T^2 \quad \text{for MB} \\ &= \frac{ge^2}{6\pi^2} \tau_c \zeta(2) T^2 = \frac{ge^2}{36} \tau_c T^2 \quad \text{for BE} \end{aligned}$$

$$= \frac{ge^2 \tau_c}{3\pi^2} \zeta(2) T^2 = \frac{ge^2 \tau_c}{18} T^2 \quad \text{for FD,} \quad (41)$$

where

$$\begin{aligned} \zeta(2) &= \frac{1}{\Gamma(2)} \int_0^\infty x^3 / (e^x - 1) \\ &= \sum_{n=1}^\infty \frac{1}{n^2} = \frac{\pi^2}{6}. \end{aligned} \quad (42)$$

From Eqs. (40) and (41), we can understand that $\eta/(\tau_c T^4)$ and $\sigma/(\tau_c T^2)$ are constant values, whose magnitude are different for different distribution function as shown by straight horizontal lines (solid line for MB, dash line for BE and dotted line for FD) in Fig 2(a), (b). Here we did not take any degeneracy factor, i.e. we keep $g = 1$. The constant value of $\eta/(\tau_c T^4)$ and $\sigma/(\tau_c T^2)$ means that shear viscosity and electrical conductivity of massless bosonic or fermionic matter are proportional to fourth power and second power of temperature respectively. Another thing is that both transport coefficients η and σ are proportional to relaxation time in $B = 0$ picture, which will be modified at $B \neq 0$ case. We will see it in next subsection.

During generation of figures in next sub-section (3.3), we did not consider spin, flavor degeneracy as well as particle anti-particle contribution. Although, for QGP system where particle anti-particle both are present, one must consider these degeneracy factors. Another point - for zero chemical potential, Hall components of shear viscosity (η_\times) and electrical conductivity (σ_\times) will vanish because Hall transport for equal number of particles and anti-particles are exactly canceled out. One should identify that Hall coefficients are odd function of τ_B , which is basically responsible for canceling the contributions between particle and anti-particle. At finite chemical potential (μ) hall components will be non-zero. In next sub-section (3.3), results are for only one species with $g = 1$ and $\mu = 0$ to focus only on each components of the transport coefficients in a magnetic field. However, in Sec. (4), instead of one species, we have considered entire plasma (massless QGP) at $\mu = 0$ with appropriate degeneracy factors, where we don't get any Hall transport coefficients.

3.3 Shear viscosity and electrical conductivity for $B \neq 0$

Let us come to $B \neq 0$ picture and applying massless case in the expressions of perpendicular and Hall-type shear viscosity and electrical conductivity components, given in Eqs. (12) or (20) and (32). Using massless relation $\mathbf{p} = \omega$ in Eqs. (12) or (20), one can obtain $\eta_{\perp, \parallel, \times}$ as

$$\begin{aligned} \eta_{\perp, \parallel} &= \tilde{\eta}_{1,2} = \eta_0, (\eta_0 + \eta_2) \\ &= \frac{\eta(B=0)}{1 + (4, 1) \times (\tau_c/\tau_B)^2} = \frac{\frac{4g \tau_c}{5\pi^2} T^4}{1 + (4, 1) \times (\tau_c/\tau_B)^2} \quad \text{for MB} \\ &= \frac{\eta(B=0)}{1 + (4, 1) \times (\tau_c/\tau_B)^2} = \frac{\frac{4g\pi^2 \tau_c}{450} T^4}{1 + (4, 1) \times (\tau_c/\tau_B)^2} \quad \text{for BE} \end{aligned}$$

$$= \frac{\eta(B=0)}{1 + (4, 1) \times (\tau_c/\tau_B)^2} = \frac{\frac{7g\pi^2 \tau_c}{900} T^4}{1 + (4, 1) \times (\tau_c/\tau_B)^2} \quad \text{for FD} \quad (43)$$

and

$$\begin{aligned} \eta_\times &= \tilde{\eta}_4 = \eta_4 \\ &= \frac{\eta(B=0)(\tau_c/\tau_B)}{1 + (\tau_c/\tau_B)^2} = \frac{\frac{4g \tau_c}{5\pi^2} (\tau_c/\tau_B) T^4}{1 + (\tau_c/\tau_B)^2} \quad \text{for MB} \\ &= \frac{\eta(B=0)(\tau_c/\tau_B)}{1 + (\tau_c/\tau_B)^2} = \frac{\frac{4g\pi^2 \tau_c}{450} (\tau_c/\tau_B) T^4}{1 + (\tau_c/\tau_B)^2} \quad \text{for BE} \\ &= \frac{\eta(B=0)(\tau_c/\tau_B)}{1 + (\tau_c/\tau_B)^2} = \frac{\frac{7g\pi^2 \tau_c}{900} (\tau_c/\tau_B) T^4}{1 + (\tau_c/\tau_B)^2} \quad \text{for FD.} \end{aligned} \quad (44)$$

For calculation simplification, we have considered average energy in τ_B (See Sec. (8.3) in Appendix)

$$\begin{aligned} \tau_B &= \omega_{\text{av}}/eB = \frac{3T}{eB} \quad \text{for MB} \\ &= \left\{ \frac{\zeta(4)}{\zeta(3)} \right\} \frac{3T}{eB} \quad \text{for BE} \\ &= \left\{ \frac{7\zeta(4)}{2\zeta(3)} \right\} \frac{3T}{eB} \quad \text{for FD.} \end{aligned} \quad (45)$$

Solving Eq. (32) for massless case, we get

$$\begin{aligned} \sigma_n &= \frac{\sigma(B=0)(\tau_c/\tau_B)^n}{1 + (\tau_c/\tau_B)^2} = \frac{\frac{ge^2 \tau_c}{3\pi^2} T^2 (\tau_c/\tau_B)^n}{1 + (\tau_c/\tau_B)^2} \quad \text{for MB} \\ &= \frac{\sigma(B=0)(\tau_c/\tau_B)^n}{1 + (\tau_c/\tau_B)^2} = \frac{\frac{ge^2 \tau_c}{36} T^2 (\tau_c/\tau_B)^n}{1 + (\tau_c/\tau_B)^2} \quad \text{for BE} \\ &= \frac{\sigma(B=0)(\tau_c/\tau_B)^n}{1 + (\tau_c/\tau_B)^2} = \frac{\frac{ge^2 \tau_c}{18} T^2 (\tau_c/\tau_B)^n}{1 + (\tau_c/\tau_B)^2} \quad \text{for FD,} \end{aligned} \quad (46)$$

where reader should keep in mind - $\sigma_\perp = \sigma_0$ and $\sigma_\times = \sigma_1$.

We have plotted $\eta_{\perp, \parallel, \times}/(\tau_c T^4)$ as a function of T and eB/m_π^2 in Fig. 2(a) and 3(a). In similar way, by putting $n = 0, 1$ in Eq. (32), we can estimate $\sigma_{\perp, \times}/(\tau_c T^4)$, whose T and eB/m_π^2 dependence are shown in Fig. 2(b) and 3(b). The $\eta_{\perp, \parallel}$ and σ_\perp increases with T and decreases with B due to increasing and decreasing of anisotropic factor $1/[1 + (4, 1) \times (\tau_c/\tau_B)^2]$, where $\tau_B \propto T/B$. However, this monotonic trend can not be obtained for Hall-type components of shear viscosity η_\times and electrical conductivity σ_\times because their anisotropic factor

$$A_\times = (\tau_c/\tau_B)/[1 + (\tau_c/\tau_B)^2] \quad (47)$$

follow a non-monotonic T, B dependence. For constant value of τ_c , $\frac{\tau_c}{\tau_B} \propto \frac{B}{T}$ and so, the anisotropic factor A_\times will increase first in the domain of $\frac{\tau_c}{\tau_B} < 1$ and then decrease in the domain of $\frac{\tau_c}{\tau_B} > 1$. Those domains can be seen in Figs. 2(c) and 3(c), where τ_B is plotted against T and

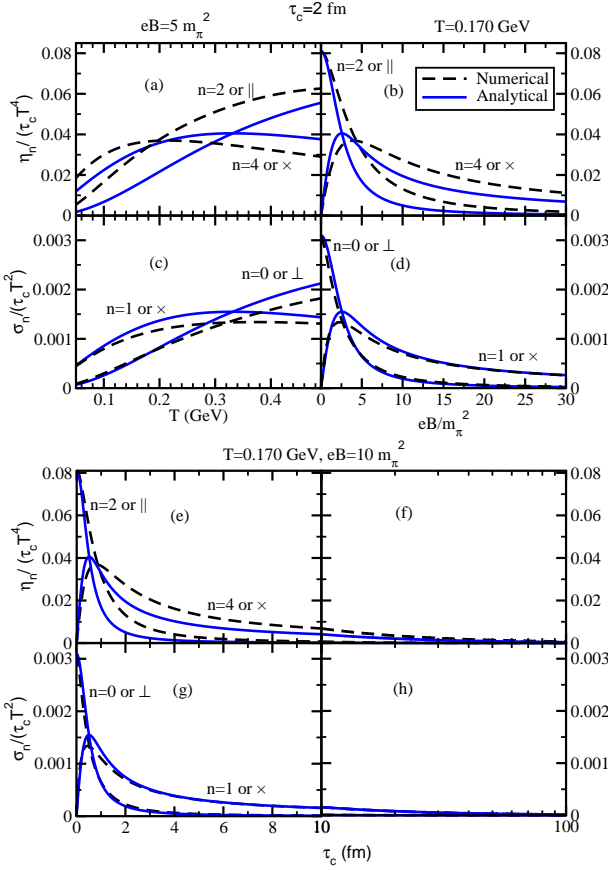


Fig. 4. Numerical values of $\eta_{2,4}/(\tau_c T^4)$ from Eqs. (12), (12), and $\sigma_{0,1}/(\tau_c T^4)$ from Eq. (32) are plotted by black dash line. Corresponding values from analytic Eqs. (43), (44) and (46) are plotted by blue solid line.

B axes and compared with $\tau_c = 2$ fm value. One should notice that the parallel component of electric conductivity is exactly same with isotropic value i.e. $\sigma_{\parallel} = \sigma$ but for shear viscosity, they are not equal, rather $\eta_{\parallel} < \eta$.

To get a simplified analytic form of $\eta_{\perp, \parallel, \times}$ and $\sigma_{\perp, \times}$, as given in Eqs. (43), (44) and (46), we have considered momentum/energy independent expression of $\tau_B = \omega_{\text{av}}/(eB)$, given in Eq. (45). However, one can obtain numerical values of $\eta_{\perp, \parallel, \times}$ from Eqs. (12) or (20), and $\sigma_{\perp, \parallel, \times}$ from Eq. (32) by using massless relation $\mathbf{p} = \omega$ and $\tau_B = \omega/(eB)$, instead of any simplified average value. These numerical and analytical results are plotted by black dash and blue solid lines in Fig. (4), where their values are quite separated but well merged at low T and/or high B and τ_c . Their merging zone is basically strong field domain, where $\tau_c/\tau_B \gg 1$ will be achieved. Qualitative T , B and τ_c dependent pattern of curves, obtained from analytic and numerical approaches are quite similar. For simplicity and getting a quick estimations, one can use analytic expressions of massless case, given by Eqs. (43), (44) and (46).

3.4 Comparison between massless expressions of $\tilde{\eta}_n$ and η_n

Let us now proceed for comparison between massless expressions of $\tilde{\eta}_n$ and η_n . There are two different possible set of independent traceless tensors, prescribed in Ref. [18] and Refs. [61,62], from where one can find $\tilde{\eta}_n$ and η_n respectively. Now if we analyze the earlier existing references, the we can find that Refs.[19,22,25,26,27,28,21] have adopted former set of tensors and calculated $\tilde{\eta}_n$, While Ref. [28,29] have adopted latter set of tensors and calculated η_n . In this context, present article has obtained both $\tilde{\eta}_n$ and η_n in RTA based kinetic theory approach and present section is aimed to explore the comparative documentation of their massless expressions. Though final expressions of $\tilde{\eta}_n$, obtained/used by Refs.[19,22,25,26,27,21] and η_n , obtained/used by Refs. [28,29] are exactly same as obtained here, but difference in approaches or mathematical steps can be found. For example, to calculate η_n Ref. [28] has gone through method of moment technique, while present work has adopted RTA based kinetic theory. On the other hand, to calculate $\tilde{\eta}_n$, Refs. [21,26] and present work both have adopted RTA based kinetic theory but one should notice the differences among their way of calculations.

To get a clear comparative picture between the expressions of $\tilde{\eta}_n$ and η_n , let us first write down their simplified (massless) structures in Table (1). They are expressed in

Table 1. Taking $\tau_c/\tau_B = x$, simplified structures of shear viscosity components, obtained from independent tensors of Ref. [18] (first column) and Refs. [61,62] (second column) are tabulated in respectively.

From tensors of Ref. [18]	From tensors of Refs. [61,62]
$\tilde{\eta}_0 = \eta$	$\eta_0 = \eta \frac{1}{1+4x^2}$
$\tilde{\eta}_1 = \eta \frac{1}{1+4x^2}$	$\eta_1 = \eta \left(\frac{16}{3} \right) \frac{x^2}{1+4x^2}$
$\tilde{\eta}_2 = \eta \frac{1}{1+x^2}$	$\eta_2 = \eta \frac{3x^2}{(1+4x^2)(1+x^2)}$
$\tilde{\eta}_3 = \eta \frac{x}{1/2+2x^2}$	$\eta_3 = \eta \frac{x}{1+4x^2}$
$\tilde{\eta}_4 = \eta \frac{x}{1+x^2}$	$\eta_3 = \eta \frac{x}{1+x^2}$

terms of $x = \tau_c/\tau_B$. The quantity $\xi_B = \tau_c(qB/T)$ of Ref. [28] and our defined quantity $x = \tau_c/\tau_B = \tau_c(qB/3T)$ for MB distribution are connected as $x = \xi_B/3$. Adjusting this proper replacement, one can find that our massless expressions of η_n are exactly same as obtained by Ref. [28], which are listed in second column of Tab. (1). Another point is that Ref. [28] has taken $\eta = \frac{4}{3}\tau_c P = \frac{4g\tau_c T^4}{3\pi^2}$, which is 5/3 times larger than Eq. (40), used here for MB distribution. The famous 1/15 factor in η , which is coming due to the identity of average momenta, given in Eq. (3), which is not considered in Ref. [28]. Instead of 1/15, they have considered 1/3 factor as a three dimensional space average. Although whatever the values of η , one can normalize it from the expressions η_n and the anisotropic factors will be our matter of interest.

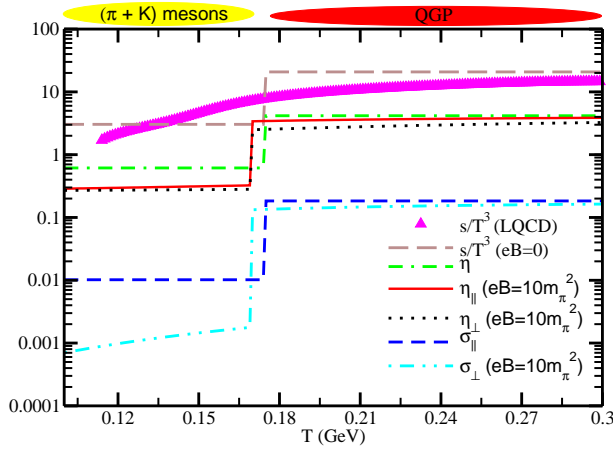


Fig. 5. Normalized values of entropy density (s/T^3), parallel and perpendicular component of shear viscosity ($\eta_{\parallel,\perp}/(\tau_c T^4)$) and electrical conductivity ($\sigma_{\parallel,\perp}/(\tau_c T^2)$) at $B = 0$ and $B = 10m_\pi^2$ for HM ($T < T_c$) and QGP ($T > T_c$) massless phases, where transition temperatures T_c are taken from Refs [4, 5].

The connection between $\tilde{\eta}_n$ and η_n are well discussed in Sec. (2.2). One can easily check those relation with the help of these massless expression, given in Table. (1).

4 Aspects of RHIC or LHC phenomenology

The mathematical anatomy of shear viscosity and electrical conductivity in presence of magnetic field, which is addressed for MB, FD and BE distribution functions in general, can have a straight forward application in RHIC or LHC matter. The massless results can provide us a rough boundary within which RHIC or LHC matter undergoes a phase transition from quark gluon plasma (QGP) state to hadronic matter (HM) state. Here we have attempted to sketch those possible boundaries of two phases in Fig. (5). Before going to transport coefficients results, we have first demonstrate the standard entropy density for calibrating our phenomenological attempt. Above transition temperature ($T > T_c$), we have considered massless QGP with (charged) quark degeneracy factors

$$\begin{aligned} g &= \text{Color} \times \text{Spin} \times \text{Particle} - \text{Antiparticle} \times \text{Flavor} \\ &= 3 \times 2 \times 2 \times 3 \\ &= 36, \end{aligned} \quad (48)$$

(neutral) gluon degeneracy factors

$$\begin{aligned} g &= \text{Color} \times \text{Spin} \\ &= 8 \times 2 \\ &= 16. \end{aligned} \quad (49)$$

On the other hand, below transition temperature ($T < T_c$), we have considered massless HM, where abundant pion and Kaon are considered only. For $B = 0$ case, we will consider hadron degeneracy factor $g = 7$ by counting pion degeneracy factors $g = 3$ and Kaon degeneracy factors $g = 4$. while for $B \neq 0$, we have to count degeneracy

factors of charged hadrons and neutral hadrons as $g = 4$ (π^+ , π^- , K^+ , K^-) and $g = 3$ (π^0 , K^0 , \bar{K}^0) respectively. We will use FD distribution results for quarks and BE distribution results for gluon and mesons. Taking care about those distributions and degeneracy factors of two phases, we have included the standard massless results of normalized entropy density s/T^3 (brown dash line) along with its lattice QCD (LQCD) results (pink triangles) [4, 5] at $B = 0$. The crossover nature of quark-hadron transition, prescribed by LQCD can be realized as a smooth transition between massless limits of two phases. So, these massless estimations might be considered as reference frames of two phases within which actual crossover transition will be occurred.

After getting calibration from s/T^3 results, let us proceed to sketch the boundaries of two phases for normalized shear viscosity ($\eta/(\tau_c T^4)$), electrical conductivity ($\sigma/(\tau_c T^2)$). At $B = 0$, they are drawn by green dash-dotted and blue dash lines, whose shape are exactly same as s/T^3 but their strengths are different only. Marking the values of their boundaries, we can write the inequalities $3.04 < \frac{s}{T^3} < 20.79$, $0.61 < \frac{\eta}{\tau_c T^4} < 4.16$, $0.01 < \frac{\sigma}{\tau_c T^2} < 0.18$ at $B = 0$ for any values of τ_c . Now when we go for $B \neq 0$ case of QGP and HM, then neutral hadrons and gluons will have same contribution in shear viscosity as they had for $B = 0$ case. However, the contribution from charged hadrons and quarks will face a suppression due to magnetic field. The net suppression values of η_\perp and η_\parallel are shown in Fig. (5) by red solid and black dotted lines respectively. The results of $\eta_\perp \neq \eta_\parallel$ indicates that anisotropy in shear transportation is developed due to magnetic field. Similarly, when we go to calculate electrical conductivity, we will find suppression of contribution from charged hadron and quarks. Unlike to shear viscosity case, here neutral hadrons and gluon will never contribute. Another difference from shear viscosity case, at finite B picture σ_\perp only suppress but σ_\parallel remain equal with σ . So, the differences between σ_\perp and σ_\parallel in QGP and HM phases basically measure the anisotropic trend of electric charge transportation. The impact of this anisotropic conductivity might disclose an anisotropic dilepton and photon productions, as one can find a proportional relation in Ref. [55]. The detail four or three momentum distribution of electromagnetic current-current correlator is basically hidden in dilepton or photons yields, whose zero momentum limit measures the electrical conductivity. That is why a straight forward expectation is a difference between dilepton or photon yields in parallel and perpendicular direction as $\sigma_\parallel \neq \sigma_\perp$. Its detail derivations are quite rigorous, so we plan it as a future project.

We have not discussed anything about Hall component η_\times and σ_\times as they are completely vanished for QGP system with zero quark chemical potential and HM system with zero baryon chemical potential. This is happened due to opposite Hall-flow of particle and anti-particle with equal strength at zero net quark/baryon density system. However, for non-zero net quark/baryon density system, one can get a non-zero Hall flow, but we have not gone

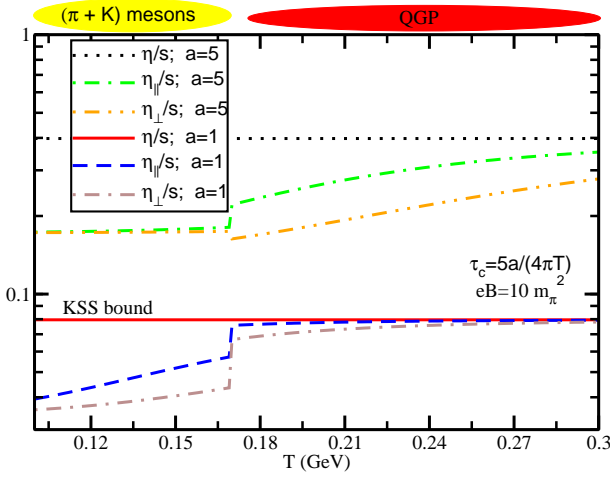


Fig. 6. Numerical bands for viscosity to entropy density ratio at $B = 0$ and $B = 10m_\pi^2$.

through that direction as our interest is focus on RHIC or LHC phenomenology.

From the massless values of thermodynamical quantities like entropy density and transport coefficients like shear viscosity, electrical conductivity for QGP and HM phases, we might get a range, within which their actual values will change. From lattice QCD (LQCD) side [4, 5], quark-hadron phase transition is realized as crossover type transition, which shows inverse magnetic catalysis (IMC) pattern near transition temperature. This fact is attempted to map from effective QCD model side [63, 64, 65] (see Ref. [63] for review). With the help of those effective QCD model, one can get rich version of estimations for $\eta_{\parallel,\perp}$, $\sigma_{\parallel,\perp}$ within the massless boundaries of two phases.

From QGP phenomenology, we know that the viscosity to entropy density ratio (η/s) is more meaningful quantity than viscosity only, as the ratio directly measures the fluid property. RHIC or LHC matter has very low η/s , close to its KSS bound - $\frac{1}{4\pi}$ [59]. To get experimental values of $\frac{\eta}{s} = \frac{a}{4\pi}$ (with $a = 1-5$) [60] for RHIC or LHC matter, $\tau_c = \frac{5a}{4\pi T}$ is expected for massless fluid, by using η from Eq. (40) and s from Eq. (38). Interestingly τ_c are same for MB, BE and FD cases, although their individual η and s expressions are different. For QGP case, we have to use the results of BE for gluon and FD for quarks with their respective degeneracy factors, which will be ultimately canceled out in ratio η/s . Hence, the phenomenological imposition to massless QGP,

$$\begin{aligned} \frac{\eta_{\text{QGP}}}{s_{\text{QGP}}} &= \frac{a}{4\pi} \\ \frac{[\frac{7}{8} \times 24 + 16] \frac{4}{5\pi^2} \tau_c \zeta(4) T^4}{[\frac{7}{8} \times 24 + 16] \frac{4}{\pi^2} \zeta(4) T^3} &= \frac{a}{4\pi} \\ \Rightarrow \tau_c &= \frac{5a}{4\pi T}, \end{aligned} \quad (50)$$

will provide us a numerical band of relaxation time $\tau_c = \frac{5}{4\pi T}$ to $\frac{25}{4\pi T}$. If we consider same calculation for massless $(\pi + K)$ system, results remain same because two massless

phases are just different by their degeneracy factors and they are exactly canceled out in η/s ratio. Therefore, two horizontal lines $\eta/s = 1/(4\pi)$ and $\eta/s = 5/(4\pi)$ at $B = 0$ are extended from QGP to HM temperature domain. However, this exact cancellation will not work for $B \neq 0$ case as shear viscosity expressions of charged and neutral particles of QGP and HM system will be different. Using this τ_c we have generated η_{\parallel}/s and η_{\perp}/s for QGP and HM system (in their respective T -zones) in Fig. (6), where blue dash, brown dash-dotted lines correspond to $\tau_c = \frac{5}{4\pi T}$ and green dash-dotted, orange dash-double-dotted lines correspond to $\tau_c = \frac{25}{4\pi T}$. We notice that the horizontal lines (red solid and black dotted lines) for $\eta/s = 1/(4\pi)$ and $5/(4\pi)$, indicating numerical band for η/s at $B = 0$, are suppressed in finite B scenario. We can understand that the suppression is mainly coming for B dependent shear viscosity of quark component in QGP temperature range ($T > T_c$) and charged hadron component in HM temperature range ($T < T_c$). Although for realistic quark-hadron crossover type transition might have a more reach T and B dependent structure but these massless values of two phases provide us a rough order of magnitude and a qualitative conclusion about the impact of B on fluid property of QGP and HM system. The present work indicates that the magnetic field might be in favor to build perfect fluid nature of RHIC or LHC matter as the ratio is suppressing at finite magnetic field picture.

5 On lower bound of viscosity to entropy density ratio

If we notice the curves of η_{\parallel}/s and η_{\perp}/s in Fig. (6) at $B \neq 0$ for $\tau_c = 5/(4\pi T) = \tau_c^0$ (say), then we can see that they come lower than KSS bound. Now according to dual holographic type theory [51, 52], parallel component can cross the bound but perpendicular can't i.e. their lower bound can be expressed as

$$\begin{aligned} \frac{\eta_{\parallel}}{s} &< \frac{1}{4\pi} \\ \frac{\eta_{\perp}}{s} &= \frac{1}{4\pi}. \end{aligned} \quad (51)$$

If we analyze the existing litterateurs on QGP [19, 22, 21, 26, 28, 29] including present work, we can't reach lower bound $\frac{\eta_{\perp}}{s} = \frac{1}{4\pi}$ by using τ_c . The reason might be as follows. The quantum description like Landau quantization version of kinetic theory approach or Kubo approach has not been considered yet. They might help to build that bound probably but it will be only confirmed if one will really enter into those calculations in future. However, one can always able to find a $\tau_c(T, B)$, for which $\frac{\eta_{\perp}}{s} = \frac{1}{4\pi}$ will be established.

Similar to $B = 0$ case, where $\tau_c^0 = 5/(4\pi T)$ is obtained by imposing $\frac{\eta}{s} = \frac{1}{4\pi}$ to massless MB/BE/FD system, we can impose

$$\frac{\eta_{\perp}}{s} = \frac{1}{4\pi}$$

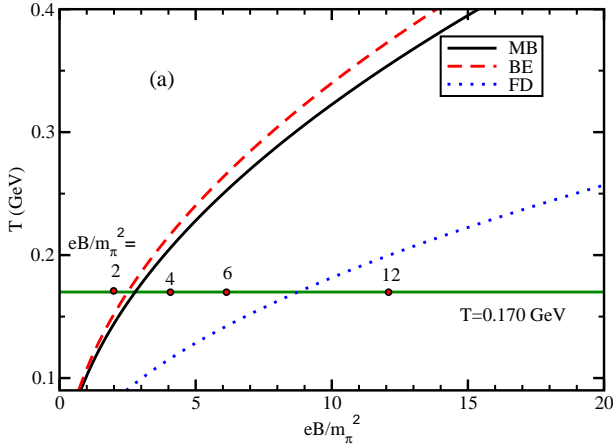


Fig. 7. $T \propto \sqrt{eB}$ curves for MB (black solid line), BE (red dash line), FD (blue dotted line) cases, below which η_{\perp}/s never touch KSS line.

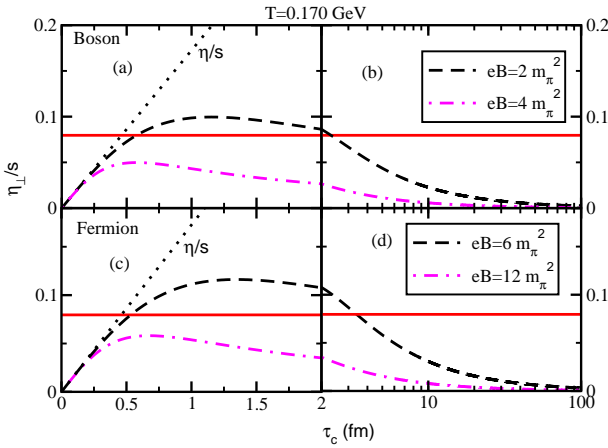


Fig. 8. η_{\perp}/s vs τ_c for bosonic (a-b) and fermionic (c-d) medium. Black dotted line is for $B = 0$ case; black dash and pink dash-dotted lines are for two finite magnetic field cases, where pink dash-dotted lines always remain below KSS bound.

$$\begin{aligned} \Rightarrow \frac{T\tau_c/5}{1 + 4(\tau_c/\tau_B)^2} &= \frac{1}{4\pi} \\ \Rightarrow \frac{\tau_c/\tau_c^0}{1 + 4(\tau_c/\tau_B)^2} &= 1, \end{aligned} \quad (52)$$

where average τ_B values for MB, BE and FD cases will be different. Above Eq. (52) will provide us a quadratic equation of τ_c :

$$\tau_c^2 - \left(\frac{\tau_B^2}{4\tau_c^0}\right)\tau_c + \frac{\tau_B^2}{4} = 0, \quad (53)$$

whose solution is

$$\tau_c = \tau_c^{\pm} = \frac{\tau_B^2}{8\tau_c^0} \left[1 \pm \sqrt{1 - 16\left(\frac{\tau_c^0}{\tau_B}\right)^2} \right]. \quad (54)$$

So far from our best knowledge, we are first time addressing an *analytic* expressions of $\tau_c(T, B)$, where massless bosonic/fermionic matter in presence of magnetic field

reach the KSS bound. To get a physical solution of Eq. (54), we need

$$\begin{aligned} 1 - 16\left(\frac{\tau_c^0}{\tau_B}\right)^2 &\geq 0 \\ \Rightarrow \tau_B &\geq 4\tau_c^0. \end{aligned} \quad (55)$$

Using MB relation $\tau_B = \frac{3T}{eB}$ in above inequality, we have

$$\begin{aligned} \frac{3T}{eB} &\geq 4\frac{5}{4\pi T} \\ T &\geq \left(\frac{5eB}{3\pi}\right)^{1/2}. \end{aligned} \quad (56)$$

Corresponding FD and BE relations from Eq. (45) will give

$$\begin{aligned} T &\geq \left[\left(\frac{\zeta(3)}{\zeta(4)}\right)\frac{5eB}{3\pi}\right]^{1/2} \text{ for BE} \\ T &\geq \left[\left(\frac{2\zeta(3)}{7\zeta(4)}\right)\frac{5eB}{3\pi}\right]^{1/2} \text{ for FD}. \end{aligned} \quad (57)$$

Drawing $T - eB$ curves of Eqs. (56) and (57) in Fig.7, one can identify upper allowed domain, where KSS bound can be achieved. On the other hand, lower domain is forbidden zone, because we will get $\eta_{\perp}/s < 1/(4\pi)$, which is not possible according to Refs. [51,52]. Or in other word, we should accept that the present massless expression of η_{\perp}/s fails to maintain its lower bound in the forbidden zones of $T-B$ plane which can also be consider as strong magnetic field zone.

To explore the fact, we have drawn straight horizontal (green solid) line at $T = 0.170$ GeV, where we have chosen points $eB = 2m_{\pi}^2$ and $eB = 4m_{\pi}^2$ in allowed and forbidden zone for bosonic medium. Similar points are $eB = 6m_{\pi}^2$ and $eB = 12m_{\pi}^2$ for fermionic medium. Generating η_{\perp}/s vs τ_c curves for bosonic medium (a-b) and fermionic (c-d) medium at those points, we can see that η_{\perp}/s always remain below KSS value at the points of forbidden zone. At the point of allowed zone, we can get solution of Eq. (54) at $\tau_c = \tau_c^{\pm}$, which can be identified by crossing points of η_{\perp}/s with KSS line (red horizontal line) in Figs. (8). We have also drawn $\eta/s \propto \tau_c$ (dotted line) curves in Figs. 8(a) and (c). Due to simple proportional nature, η/s will cross KSS line at one point ($\tau_c = \tau_c^0$), but η_{\perp}/s cross the KSS line in two points ($\tau_c = \tau_c^{2\pm}$) because of non-monotonic relation $\eta_{\perp}/s \propto \frac{\tau_c}{1 + 4(\tau_c/\tau_B)^2}$. We notice that τ_c^0 and τ_c^{\pm} are little close in numerical values and both signify the lower values of τ_c , for which viscosity to entropy density ratio touch its KSS bound. Interestingly, we are getting an upper value of τ_c (τ_c^+), where η_{\perp}/s again reach its KSS bound. This fact is completely new fact, appeared in the picture of finite magnetic field.

Above graphical discussion give us an idea about allowed/forbidden $T-B$ domain, where τ_c parameter can/can't tune η_{\perp}/s to $1/(4\pi)$. Now, let us draw $\tau_c^{\pm}(T, B)$ along with $\tau_c^0(T)$ in Fig. (9) by using Eqs. (54). We have filtered out unphysical points of $\tau_c^{\pm}(T, B)$. Fig. 9(a), (c) shows τ_c^+ increases with T and decreases with B , whereas τ_c^- follow a mild decrement (increment) with T (B) as show in

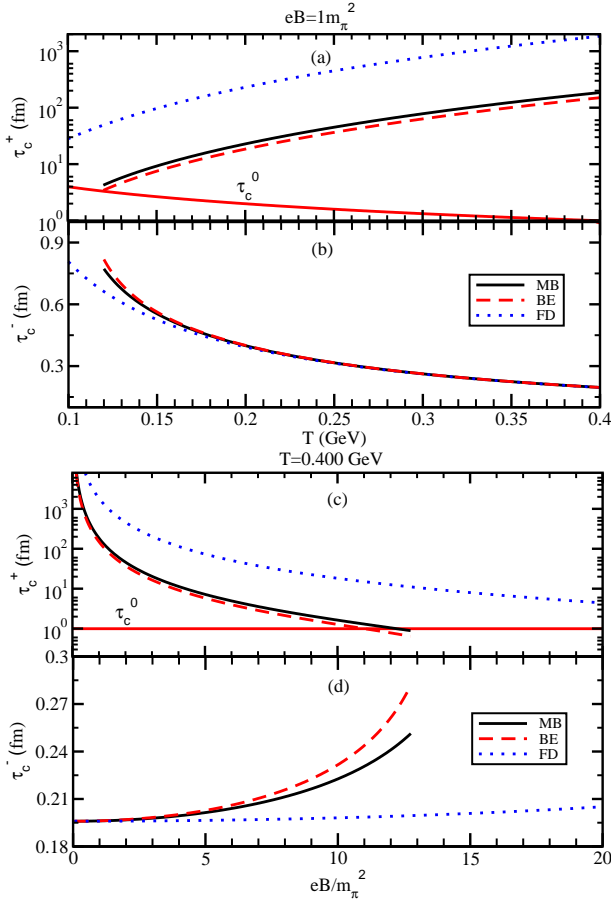


Fig. 9. T (a, b) and eB/m_π^2 (c, d) dependence of τ_c^+ (a, b), τ_c^- (c, d) for MB, BE, FD cases.

Fig. 9(b), (d). Hence, using τ_c^\pm , given in Eq. (54), we get lower bound relations

$$\begin{aligned}
 \frac{\eta_\perp}{s} &= \frac{1}{4\pi} \\
 \frac{\eta_\parallel}{s} &= \frac{\tau_c^\pm T/5}{1 + \left(\frac{\tau_c^\pm}{\tau_B}\right)^2} \\
 &= \frac{1}{4\pi} \frac{1}{\left[1 + \left(\frac{\tau_B}{\tau_c^\pm}\right)^2\right] \left[1 \pm \sqrt{1 - 16\left(\frac{\tau_c^0}{\tau_B}\right)^2}\right]} \\
 &< \frac{1}{4\pi}, \tag{58}
 \end{aligned}$$

whose qualitative dependence are quite agreements with dual holographic type results [51, 52].

Now, from fig. 7 it is clear that our proposed expression $\tau_c^\pm(T, B)$ does not have any existence in strong field ($T^2/eB \ll 1$) zone or forbidden zone. It might be considered as drawback of our proposed expressions. Therefore, checking strong field approximation, proposed by Refs. [51, 52],

$$\frac{\eta_\parallel}{s} \approx \pi \frac{T^2}{qB}, \tag{59}$$

is not possible from our proposed picture. However, one can easily check the opposite limit - weak magnetic field and/or high temperature, which is allowed by all three types of distributions - MB, BE, FD. In this limit, $eB/T^2 \ll 1$, i.e. $\tau_c^0/\tau_B \ll 1$ and Eq. (54) can be approximate as,

$$\begin{aligned}
 \tau_c^+ &\approx \frac{\tau_B^2}{4\tau_c^0} \rightarrow \infty; \\
 \tau_c^- &\approx \tau_c^0. \tag{60}
 \end{aligned}$$

So one can get back our earlier lower bound of $B = 0$ picture:

$$\frac{\eta_\parallel}{s} \rightarrow \frac{1}{4\pi} \leftarrow \frac{\eta_\perp}{s}. \tag{61}$$

6 Summary

In summary, we have explored the shear viscosity and electrical conductivity calculations for bosonic and fermionic medium, facing an external magnetic field. Unlike to one shear viscosity coefficients in field-free picture, 5 shear viscosity coefficients will come into the picture, when an external magnetic field is applied to the medium. This is because 5 independent velocity gradient tensors can be designed in presence of magnetic field and connecting them with the viscous stress tensor, one can get 5 proportional constants, which can be recognized as shear viscosity coefficients (by definition). After going through the existing literateurs on the relation between viscous stress tensor and 5 velocity gradient tensors at finite magnetic field, we have found two sets of tensor structures. One is proposed from Ref. [18] and another is designed by Refs. [61, 62].

Starting from both sets of tensors one by one, present work has obtained two sets of expressions for 5 shear viscosity coefficients, whose inter-connecting relations are discussed and they have been ultimately classified into three basic components - parallel, perpendicular and Hall components as one get same for electrical conductivity at finite magnetic field. Although, one should keep in mind that former is defined for four rank tensor, while latter is defined for two rank tensor. We have adopted kinetic theory approach in relaxation time approximation. For field-free picture, connecting the macroscopic (hydrodynamic) and microscopic (kinetic theory based) structures of viscous stress tensors, one can obtain the shear viscosity expression, where a proportional dependence with relaxation time is established in microscopic structure with the help of RTA based Boltzmann equation. At finite magnetic field, repeating same mathematical steps, we have obtained 2 sets of 5 shear viscosity components, whose final expressions are in well agreements with earlier references although a difference in methodology or steps can be clearly noticed.

After derivation of expressions, we have presented the parallel, perpendicular and Hall components of shear viscosity and electrical conductivity for massless bosonic and fermionic matter, which will be controlled by their own distribution functions - Bose-Einstein and Fermi-Dirac. We have also included the case of Maxwell-Boltzmann

distribution functions. In external magnetic field, a magnetic time scale for cyclotron motion of charge particle in the medium is introduced along with relaxation time scale. The competition between these two time scale basically create anisotropic transportation in the medium, for which many components are found. Mainly the values of parallel and perpendicular components will be different at finite magnetic field. At zero field limits, their values will be merged to their isotropic value. Taking average energy approximation in magnetic time scale, we get analytic expressions for all components of shear viscosity and electrical conductivity, which are little deviated from exact numerical values but their qualitative trends remain same. So, for quick estimations, the analytic expressions can be used by the research community. perpendicular component always reduce with magnetic field and enhance with temperature, while Hall component follow a non-monotonic trend with temperature and magnetic field.

Using these massless results of viscosity and conductivity of Fermionic and Bosonic medium to quark gluon plasma and hadronic matter system for zero quark/baryon chemical potential, we have obtained their parallel and perpendicular components, where particle and anti-particle distributions are simply added. Being odd function of electric charge, Hall components will be zero as particle and anti-particle contributions are exactly canceled out. One can get its non-zero values for non-zero quark/baryon chemical potential. The massless results of quark gluon plasma and hadronic matter phases can provide us a rough order of strength, within which actual results will vary during (crossover type) quark-hadron phase transition. Our results show a suppression of parallel and perpendicular components of shear viscosity as well as viscosities to entropy density ratio due to magnetic field with respect to their isotropic value for zero magnetic field case. It indicates that magnetic field might be in favor of building perfect fluid nature in RHIC or LHC matter. For electrical conductivity, perpendicular component face similar suppression but parallel component remain unaffected. Also two components have different values, which reflect the anisotropic transportation due to magnetic field and they might have some phenomenological impact, for which a further rigorous research might be necessary. One of the possibilities might be to search anisotropic dilepton or photon production as they have direct link with conductivity. We have also attempted to connect our viscosity to entropy density ratio along parallel and perpendicular direction with their lower bounds, expected from dual holographic type theory. Imposition of this connection provide an expressions of relaxation time as a function of temperature and magnetic field, for which lower bound expectation can be achieved.

Our calculation is completely based on classical picture, although we have considered Fermi-Dirac and Bose-Einstein distribution, which might be considered as quantum aspect of statistical mechanics. So we might call this description as semi-classical framework. However, complete quantum mechanical description by considering Lan-

dau levels of charge particle of medium can be considered as its immediate extension of present framework, which we are planning for future studies.

Acknowledgment: JD and SG acknowledge to MHRD funding via IIT Bhilai. PM thanks for (payment-basis) hospitality from IIT Bhilai during his summer internship tenure (May-June, 2019).

7 Appendix: C_n calculations

7.1 For tensors of Refs. [18]

The detail calculations of C_n for traceless independent tensors of Refs. [18] from the RTA based RBE, given in Eq.(10) will be documented in this section.

For zero bulk viscosity and knowing that the tensors V_{ij} is symmetric, b_{ij} is anti-symmetric in i, j we get some relations: $\nabla \cdot \mathbf{V} = V_{ii} = 0$, $V_{ij}b_j = 0$, $b_{ij}b_i = b_{ij}b_j = 0$, $b_{ij}v_i v_j = 0$. Using the above conditions, Eq. (10) takes the form,

$$\begin{aligned} \frac{\omega}{T} v_i v_j V_{ij} f_0 (1 - a f_0) = & -\frac{2}{\tau_B} \left[C_1 \left\{ 2V_{ik} b_{ij} v_j v_k \right. \right. \\ & \left. \left. - 2V_{ik} b_{ij} b_k v_j (\mathbf{v} \cdot \mathbf{b}) \right\} \right. \\ & + C_2 \left\{ 2V_{ik} b_{ij} v_j b_k (\mathbf{v} \cdot \mathbf{b}) \right\} \\ & + C_3 \left\{ 2V_{ij} v_i v_j - 4V_{ij} v_i b_j (\mathbf{v} \cdot \mathbf{b}) \right\} \\ & + C_4 \left\{ 2V_{ij} v_i b_j (\mathbf{v} \cdot \mathbf{b}) \right\} \left. \right] \\ & + \frac{1}{\tau_c} \left[C_1 \left\{ 2V_{ij} v_i v_j - 4V_{ij} v_i b_j (\mathbf{v} \cdot \mathbf{b}) \right\} \right. \\ & + C_2 \left\{ 4V_{ij} v_i b_j (\mathbf{v} \cdot \mathbf{b}) \right\} \\ & + C_3 \left\{ 2V_{ik} b_{jk} v_i v_j - 2V_{ij} b_{ki} b_j v_k (\mathbf{v} \cdot \mathbf{b}) \right\} \\ & \left. + C_4 \left\{ 4V_{ij} b_{ki} b_j v_k (\mathbf{v} \cdot \mathbf{b}) \right\} \right] \quad (62) \end{aligned}$$

Now, from eq. (62) comparing the following tensor structures,

$$V_{ij} v_i v_j :$$

$$-\frac{\omega}{T} f_0 (1 - a f_0) = \frac{4}{\tau_B} C_3 - \frac{2}{\tau_c} C_1 \quad (63)$$

$$V_{ij} b_{ik} v_k v_j :$$

$$\frac{4}{\tau_B} C_1 + \frac{2}{\tau_c} C_3 = 0 \quad (64)$$

$$V_{ij} b_{ik} v_k b_j (\mathbf{v} \cdot \mathbf{b}) :$$

$$\frac{2}{\tau_B} (-2C_1 + 2C_2) + \frac{1}{\tau_c} (-2C_3 + 4C_4) = 0 \quad (65)$$

$$V_{ij} v_i b_j (\mathbf{v} \cdot \mathbf{b}) :$$

$$\frac{2}{\tau_B} (-4C_3 + 2C_4) - \frac{1}{\tau_c} (-4C_1 + 4C_2) = 0 \quad (66)$$

Solving above four equations we finally get C s as,

$$\begin{aligned} C_1 &= -\frac{\omega}{2T} \frac{\tau_c}{4 \left\{ \frac{1}{4} + (\tau_c/\tau_B)^2 \right\}} f_0(1 - af_0) \\ C_2 &= -\frac{\omega}{2T} \frac{\tau_c}{1 + (\frac{\tau_c}{\tau_B})^2} f_0(1 - af_0) \\ C_3 &= -\frac{\omega}{2T} \frac{\tau_c (\frac{\tau_c}{\tau_B})}{2 \left\{ \frac{1}{4} + (\tau_c/\tau_B)^2 \right\}} f_0(1 - af_0) \\ C_4 &= -\frac{\omega}{2T} \frac{\tau_c (\frac{\tau_c}{\tau_B})}{1 + (\frac{\tau_c}{\tau_B})^2} f_0(1 - af_0) \end{aligned} \quad (67)$$

7.2 For tensors of Refs. [61,62]

Here, C_n 's for tensor of eq. 19[61,62] will be calculated.

Using C_{ij} s of Eq. (19) in Eq. (10) with tensor identities used in above subsection we get,

$$\begin{aligned} \frac{\omega}{T} v_i v_j V_{ij} f_0 (1 - af_0) &= -\frac{2}{\tau_B} \left[C_0 (2V_{ik} b_{ij} v_j v_k) \right. \\ &+ C_2 \left\{ 2V_{ik} b_{ij} v_j b_k (\mathbf{v} \cdot \mathbf{b}) \right\} \\ &+ C_3 \left\{ 4V_{ij} v_i v_j - 8V_{ij} v_i b_j (\mathbf{v} \cdot \mathbf{b}) \right\} \\ &+ C_4 \left\{ 2V_{ij} v_i b_j (\mathbf{v} \cdot \mathbf{b}) \right\} \\ &+ \frac{1}{\tau_c} \left[C_0 (2V_{ij} v_i v_j) \right. \\ &+ C_2 \left\{ 4V_{ij} v_i b_j (\mathbf{v} \cdot \mathbf{b}) \right\} \\ &+ C_3 \left\{ 4V_{ik} b_{jk} v_i v_j - 4V_{ij} b_{ki} b_j v_k (\mathbf{v} \cdot \mathbf{b}) \right\} \\ &+ C_4 \left\{ 4V_{ij} b_{ki} b_j v_k (\mathbf{v} \cdot \mathbf{b}) \right\} \left. \right] \end{aligned} \quad (68)$$

Now, from eq. (68) comparing the following tensor structures,

$V_{ij} v_i v_j :$

$$-\frac{\omega}{T} f_0(1 - af_0) = \frac{8}{\tau_B} C_3 - \frac{2}{\tau_c} C_0 \quad (69)$$

$V_{ij} b_{ik} v_k v_j :$

$$\frac{4}{\tau_B} C_0 + \frac{4}{\tau_c} C_3 = 0 \quad (70)$$

$V_{ij} b_{ik} v_k b_j (\mathbf{v} \cdot \mathbf{b}) :$

$$\frac{2}{\tau_B} (2C_2) + \frac{1}{\tau_c} (-4C_3 + 4C_4) = 0 \quad (71)$$

$V_{ij} v_i b_j (\mathbf{v} \cdot \mathbf{b}) :$

$$\frac{2}{\tau_B} (-8C_3 + 2C_4) - \frac{1}{\tau_c} (4C_2) = 0 \quad (72)$$

Solving above four equations we finally get C s as,

$$\begin{aligned} C_0 &= -\frac{\omega}{2T} \frac{\tau_c}{\{1 + 4(\tau_c/\tau_B)^2\}} f_0(1 - af_0) \\ C_2 &= -\frac{\omega}{2T} \frac{3 \tau_c (\tau_c/\tau_B)^2}{\{1 + (\tau_c/\tau_B)^2\} \{1 + 4(\tau_c/\tau_B)^2\}} f_0(1 - af_0) \\ C_3 &= -\frac{\omega}{2T} \frac{\tau_c (\tau_c/\tau_B)}{\{1 + 4(\tau_c/\tau_B)^2\}} f_0(1 - af_0) \\ C_4 &= -\frac{\omega}{2T} \frac{\tau_c (\tau_c/\tau_B)}{1 + (\tau_c/\tau_B)^2} f_0(1 - af_0) \end{aligned} \quad (73)$$

8 Appendix: massless results

8.1 Thermodynamics of massless quark at $B = 0$

Here we have shown explicit calculation of energy density, pressure and entropy density for quasi particle system considering mass $m = 0$ for MB, BE, FD at $B = 0$.

Thermal distribution function can be written in a general way in the form

$$f = \frac{1}{e^{\beta E} + a} \quad (74)$$

where, $a = 0$ for MB, $a = 1$ for FD and $a = -1$ for BE statistics.

BE: Energy density for bosons is given by

$$\epsilon = g \int_0^\infty \frac{d^3 p}{(2\pi)^3} \frac{E}{e^{\beta E} - 1} \quad (75)$$

Here $E = p$ which gives us

$$dp = dE$$

and the integral becomes

$$\begin{aligned} \epsilon &= g \int_0^\infty \frac{4\pi E^3 dE}{(2\pi)^3} \frac{1}{e^{\beta E} - 1} \\ &= g \int_0^\infty \frac{E^3 dE}{2\pi^2} \frac{1}{e^{\beta E} - 1} \end{aligned} \quad (76)$$

Substituting $\beta E = x$ giving

$$dE = \frac{dx}{\beta}$$

gives us

$$\epsilon = \frac{g_b}{2\pi^2 \beta^4} \int_0^\infty \frac{x^3 dx}{e^x - 1} \quad (77)$$

This integral can be converted into a $\zeta(s)$ function by using

$$\zeta(s) = \frac{1}{\Gamma(s)} \int_0^\infty \frac{x^{s-1} dx}{e^x - 1} \quad (78)$$

where $\Gamma(s)$ is the gamma function.

$$\begin{aligned}\epsilon &= g \times \frac{(k_B T)^4}{2\pi^2} \zeta(4) \Gamma(4) \\ &= g \frac{\pi^2}{30} T^4\end{aligned}\quad (79)$$

Using $\zeta(4) = \frac{\pi^4}{90}$ and $\Gamma(4) = 3!$ The corresponding pressure density is

$$P = \frac{\epsilon}{3} = g T^4 \frac{\pi^2}{90} \quad (80)$$

The entropy density is

$$s = \frac{\epsilon + P}{T} = \frac{4g\pi^2}{90} T^3$$

FD: Energy density for fermion is

$$\epsilon = g \int \frac{d^3p}{(2\pi)^3} E \frac{1}{e^{\beta E} + 1} \quad (81)$$

$E = p$ which gives the integral

$$\epsilon = \frac{g}{2\pi^2} \int_0^\infty \frac{E^3 dE}{e^{\beta E} + 1} \quad (82)$$

Substituting $\beta E = x$ we get

$$dE = \frac{dx}{\beta}$$

$$\begin{aligned}\epsilon &= \frac{g}{2\pi^2} T^4 \Gamma(4) \left(1 - \frac{1}{2^{4-1}}\right) \zeta(4) \\ &= \frac{7}{8} g \frac{\pi^2}{30} T^4\end{aligned}\quad (83)$$

Pressure density of fermions is given by

$$P = \frac{\epsilon}{3} = \frac{7}{8} g \frac{\pi^2}{90} T^4 \quad (84)$$

The entropy density is given by

$$s = \frac{\epsilon + P}{T} = \frac{7g\pi^2}{90} T^3$$

MB: For the Maxwell Boltzmann distribution the energy density is given by

$$\epsilon = g \int_0^\infty \frac{d^3p}{(2\pi)^3} \frac{E}{e^{\beta E}} \quad (85)$$

Since $E = p$ the energy density calculated by changing the integral to a beta function is

$$\epsilon = \frac{3gT^4}{\pi^2} \quad (86)$$

The pressure density is $P = \frac{\epsilon}{3}$

$$P = \frac{g}{\pi^2} T^4 \quad (87)$$

The entropy density is given by

$$s = \frac{\epsilon + P}{T} = \frac{4g}{\pi^2} T^3 \quad (88)$$

8.2 Shear viscosity and electrical conductivity of massless quark at $B = 0$

Here we have shown details derivation of $\eta(T)$ and $\sigma(T)$ for MB, BE, FD at $B = 0$ for massless quasi particle system. The shear viscosity η for bosons is given by

$$\eta = \frac{g\beta}{15} \int \frac{d^3p}{(2\pi)^3} \frac{p^4}{E^2} \tau_c f_0 (1 + f_0) \quad (89)$$

Here $E = p$ which gives us

$$\eta = \frac{g\beta}{15} \frac{\tau_c}{2\pi^2} \int_0^\infty p^4 dp f_0 (1 + f_0) \quad (90)$$

The shear viscosity for fermions is given by

$$\begin{aligned}\eta &= \frac{g\beta}{15} \int \frac{4\pi p^2 dp}{(2\pi)^3} p^2 \tau_c f_0 (1 - f_0) \\ &= \frac{g\beta}{15} \frac{\tau_c}{2\pi^2} \int_0^\infty p^4 dp f_0 (1 - f_0)\end{aligned}\quad (91)$$

The above 2 expressions are written as

$$\eta = A \int_0^\infty p^4 dp f_0 (1 - f_0) = AI_1 \quad (92)$$

for fermions and

$$\eta = A \int_0^\infty p^4 dp f_0 (1 + f_0) = AI_2 \quad (93)$$

for bosons. where the constant A is the substitution for

$$A = \frac{g\beta}{30\pi^2} \tau_c \quad (94)$$

The I_1 integral is evaluated as follows

$$I = \int_0^\infty p^4 dp f_0 (1 - f_0) \quad (95)$$

where $f_0 = \frac{1}{e^{\beta E} + 1} = \frac{1}{e^{\beta p} + 1}$ is the distribution function for fermions.

$$\begin{aligned}I_1 &= \int_0^\infty p^4 dp \frac{1}{e^{\beta p} + 1} \left[1 - \frac{1}{e^{\beta p} + 1}\right] \\ &= \int_0^\infty p^4 dp \frac{e^{\beta p}}{(e^{\beta p} + 1)^2} \\ &= -\frac{\partial}{\partial \beta} \int_0^\infty \frac{p^3}{e^{\beta p} + 1} dp\end{aligned}\quad (96)$$

By using the definition of $d(s)$ and $\zeta(s)$ function we solve the above integral as

$$\begin{aligned}I_1 &= -\frac{\partial}{\partial \beta} \frac{\Gamma(4)}{(\beta)^4} \left(1 - \frac{1}{2^3}\right) \zeta(4) \\ &= -\frac{\partial}{\partial \beta} \frac{3!}{\beta^4} \frac{7}{8} \zeta(4) \\ &= \frac{4!}{\beta^5} \zeta(4) \frac{7}{8}\end{aligned}\quad (97)$$

Thus

$$\eta|_{fermions} = A \frac{4!}{\beta^5} \zeta(4) \frac{7}{8}$$

The integral for Bosons is

$$\begin{aligned} I_2 &= \int_0^\infty p^4 dp \left(\frac{1}{e^{\beta p} - 1} \right) \left(1 + \frac{1}{e^{\beta p} - 1} \right) \\ &= \int_0^\infty p^4 dp \frac{e^{\beta p}}{(e^{\beta p} - 1)^2} \\ &= -\frac{\partial}{\partial \beta} \int_0^\infty p^3 dp \frac{e^{\beta p}}{e^{\beta p} - 1} \end{aligned} \quad (98)$$

Substituting $\beta p = x$ we get

$$I_2 = -\frac{\partial}{\partial \beta} \left(\int_0^\infty dx \frac{x^3}{\beta^4 (e^x - 1)} \right) \quad (99)$$

Using the definition of $\zeta(s)$ the integral is calculated as

$$I_2 = \frac{4}{\beta^5} \Gamma(4) \zeta(4) \quad (100)$$

$\eta|_{Bosons}$ is obtained as

$$\eta|_{Bosons} = A \frac{4}{\beta^5} \Gamma(4) \zeta(4) \quad (101)$$

For Maxwell-Boltzmann distribution the shear viscosity is obtained as follows

$$\eta = \frac{g\beta}{15} \int \frac{d^3 p}{(2\pi)^3} p^2 f_0 \tau_c \quad (102)$$

where $f_0 = e^{-\beta E}$ and here $E = p$.

$$\begin{aligned} \eta &= A \int_0^\infty p^4 dp e^{-\beta p} \\ &= \frac{A}{\beta^5} \int_0^\infty e^{-x} x^4 dx \\ &= \frac{A}{\beta^5} \Gamma(5) \end{aligned} \quad (103)$$

where $A = \frac{g\beta}{30\pi^2} \tau_c$ and $\Gamma(5) = 4!$

Electrical Conductivity σ for different distributions is calculated as follows:

MB: For Maxwell-Boltzmann distribution electrical conductivity is

$$\begin{aligned} \sigma &= \frac{q^2 g \beta}{3} \int \frac{d^3 p}{(2\pi)^3} \frac{p^2}{E^2} \tau_c f_0 \\ &= \frac{q^2 g \beta}{3} \int \frac{4\pi p^2 dp}{(2\pi)^3} \tau_c f_0 \end{aligned} \quad (104)$$

The distribution function is $f_0 = e^{-\beta p}$ for Maxwell-Boltzmann distribution.

$$\sigma = \frac{q^2 g \beta}{3(2\pi^2)} \int_0^\infty p^2 dp [\tau_c e^{-\beta p}] \quad (105)$$

Substituting $\beta p = x$ we get

$$\begin{aligned} \sigma &= \frac{q^2 g \beta}{3(2\pi^2)} \tau_c \int_0^\infty \frac{1}{\beta^3} dx x^2 e^{-x} \\ &= \frac{q^2 g \beta}{3(2\pi^2)} \frac{2!}{\beta^3} \tau_c \\ &= q^2 \frac{g}{3\pi^2} \frac{\tau_c}{\beta^2} \end{aligned} \quad (106)$$

FD: The electrical conductivity of fermions is given by

$$\sigma = q^2 \frac{g\beta}{3} \int \frac{d^3 p}{(2\pi)^3} \frac{p^2}{E^2} \tau_c f_0 (1 - f_0) \quad (107)$$

where the distribution function of fermions is given by

$$f_0 = \frac{1}{e^{\beta p} + 1}$$

$$\begin{aligned} \sigma &= q^2 \frac{g\beta}{3} \int_0^\infty \frac{4\pi p^2}{(2\pi)^3} dp \times \tau_c \frac{e^{\beta p}}{(e^{\beta p} + 1)^2} \\ &= \frac{q^2 g \beta}{3 \times 2\pi^2} \int_0^\infty p^2 dp \frac{e^{\beta p}}{(e^{\beta p} + 1)^2} \tau_c \end{aligned} \quad (108)$$

Using the definition of $\zeta(s)$ the integral is evaluated to be

$$\sigma = \frac{q^2 g}{2 \times 2\pi^2} \frac{1}{\beta^2} \frac{\Gamma(4)}{4} \zeta(3) \tau_c \quad (109)$$

where $\Gamma(4) = 3!$

BE: For bosons σ is

$$\sigma = \frac{q^2 g \beta}{3} \int \frac{d^3 p}{(2\pi)^3} \frac{p^2}{E^2} f_0 (1 + f_0) \tau_c \quad (110)$$

where the distribution function of bosons is given by

$$f_0 = \frac{1}{e^{\beta p} - 1}$$

$$\begin{aligned} \sigma &= \frac{q^2 g \beta}{3 \times 2\pi^2} \int_0^\infty \frac{p^2 e^{\beta p}}{(e^{\beta p} - 1)^2} dp \tau_c \\ &= \frac{q^2 g \beta}{3 \times 2\pi^2} \times I \times \tau_c \end{aligned} \quad (111)$$

where the integral I is given by

$$I = \int_0^\infty \frac{p^2 e^{\beta p}}{(e^{\beta p} - 1)^2} dp \quad (112)$$

is solved as follows

$$\begin{aligned}
I &= -\frac{\partial}{\partial\beta} \int_0^\infty \frac{p}{e^{\beta p} - 1} dp \\
&= -\frac{\partial}{\partial\beta} \left(\frac{1}{\beta^2} \right) \int_0^\infty \frac{x}{e^x - 1} dx \\
&= \frac{2}{\beta^3} \int_0^\infty \frac{x}{e^x - 1} dx \\
&= \frac{2}{\beta^3} \zeta(2) \Gamma(2) = \frac{2}{\beta^3} \zeta(2)
\end{aligned} \tag{113}$$

Putting this in the expression for conductivity we get

$$\sigma = \frac{q^2 g \beta}{3 \times 2\pi^2} \frac{2}{\beta^3} \zeta(2) \tau_c \tag{114}$$

8.3 Thermal average Energy

The expressions of viscosity and conductivity contain magnetic relaxation time τ_B which is $\tau_B = \frac{E}{qB}$. But for simplicity of calculation we will consider average energy for τ_B calculation. So, $\tau_B = \frac{\langle E \rangle}{qB}$

MB: Average energy for Maxwell Boltzmann distribution with $E = p$

$$\begin{aligned}
\langle E \rangle &= \frac{\int \frac{d^3 p}{(2\pi)^3} E e^{-\beta E}}{\int \frac{d^3 p}{(2\pi)^3} e^{-\beta E}} \\
&= \frac{\int_0^\infty p^3 dp e^{-\beta p}}{\int_0^\infty p^2 e^{-\beta p} dp} \\
&= \frac{\frac{6}{\beta^4}}{\frac{2}{\beta^3}} = \frac{3}{\beta}
\end{aligned} \tag{115}$$

FD: Average energy for fermions is

$$\begin{aligned}
\langle E \rangle &= \frac{\int \frac{d^3 p}{(2\pi)^3} E \frac{1}{e^{\beta E} + 1}}{\int \frac{d^3 p}{(2\pi)^3} \frac{1}{e^{\beta E} + 1}} \\
&= \frac{\int_0^\infty \frac{p^3 dp}{e^{\beta p} + 1}}{\int_0^\infty \frac{p^2 dp}{e^{\beta p} + 1}}
\end{aligned} \tag{116}$$

Using the definition of $\zeta(s)$ and substituting $\beta p = x$ the above integral is evaluated as

$$\begin{aligned}
\langle E \rangle &= \frac{\frac{\Gamma(4)}{\beta^4} \left(1 - \frac{1}{2^{4-1}}\right) \zeta(4)}{\frac{\Gamma(3)}{\beta^3} \left(1 - \frac{1}{2^{3-1}}\right) \zeta(3)} \\
&= \frac{7}{2} T \frac{\zeta(4)}{\zeta(3)}
\end{aligned} \tag{117}$$

BE: Average energy of Bosons with $E = p$

$$\begin{aligned}
\langle E \rangle &= \frac{\int \frac{d^3 p}{(2\pi)^3} \frac{E}{(e^{\beta E} - 1)}}{\int \frac{d^3 p}{(2\pi)^3} \frac{1}{(e^{\beta E} - 1)}} \\
&= \frac{\int_0^\infty \frac{p^3 dp}{(e^{\beta p} - 1)}}{\int_0^\infty \frac{p^2 dp}{(e^{\beta p} - 1)}}
\end{aligned} \tag{118}$$

Using the definition of $\zeta(s)$ and the substitution $\beta p = x$ the integral can be solved as

$$\langle E \rangle = \frac{1}{\beta} \frac{\zeta(4) \Gamma(4)}{\zeta(3) \Gamma(3)} \tag{119}$$

References

1. I. A. Shovkovy, Lect. Notes Phys. **871**, 13 (2013), arXiv:1207.5081 [hep-ph].
2. A. Bzdak and V. Skokov, Phys. Lett. B **710**, 171 (2012) doi:10.1016/j.physletb.2012.02.065 [arXiv:1111.1949 [hep-ph]].
3. M. D'Elia, Lect. Notes Phys. **871**, 181 (2013), arXiv:1209.0374 [hep-lat].
4. G.S. Bali, F. Bruckmann, G. Endrodi, Z. Fodor, S.D. Katz, and A. Schafer, Phys. Rev. D **86**, 071502(R), 2012.
5. G.S. Bali, F. Bruckmann, G. Endrodi, S.D. Katz, A. Schafer, J. High Energ. Phys. **1408** (2014) 177.
6. N. Mueller, J. A. Bonnet, and C. S. Fischer, Phys. Rev. D **89**, 094023 (2014), arXiv:1401.1647 [hep-ph].
7. V. A. Miransky and I. A. Shovkovy, Physics Reports **576**, 1-209 (2015), arXiv:1503.00732 [hep-ph].
8. Jens O. Andersen, William R. Taylor and Anders Tranberg, Rev. Mod. Phys. **88**, **025001**(2016), arxiv:1411:7176
9. K. Tuchin, Adv. High Energy Phys. **2013**, 490495 (2013) doi:10.1155/2013/490495 [arXiv:1301.0099 [hep-ph]].
10. W. T. Deng and X. G. Huang, Phys. Rev. C **85**, 044907 (2012) doi:10.1103/PhysRevC.85.044907 [arXiv:1201.5108 [nucl-th]].
11. D. Satow, Phys. Rev. D **90**, no. 3, 034018 (2014) doi:10.1103/PhysRevD.90.034018 [arXiv:1406.7032 [hep-ph]].
12. V. Skokov, A. Illarionov and V. Toneev, Int. J. Mod. Phys. **A 24**, 5925 (2009)
13. V. Roy, S. Pu, L. Rezzolla and D. Rischke, Phys. Lett. B **750**, 45 (2015) doi:10.1016/j.physletb.2015.08.046 [arXiv:1506.06620 [nucl-th]].
14. S. Pu, V. Roy, L. Rezzolla and D. H. Rischke, Phys. Rev. D **93**, no. 7, 074022 (2016) doi:10.1103/PhysRevD.93.074022 [arXiv:1602.04953 [nucl-th]].
15. M. Hongo, Y. Hirono and T. Hirano, arXiv:1309.2823 [nucl-th].
16. G. Inghirami, L. Del Zanna, A. Beraudo, M. H. Moghadam, F. Becattini and M. Bleicher, Eur. Phys. J. C **76**, no. 12, 659 (2016) doi:10.1140/epjc/s10052-016-4516-8 [arXiv:1609.03042 [hep-ph]].
17. S. K. Das, S. Plumari, S. Chatterjee, J. Alam, F. Scardina and V. Greco, Phys. Lett. B **768**, 260 (2017) doi:10.1016/j.physletb.2017.02.046 [arXiv:1608.02231 [nucl-th]].
18. E.M. Lifshitz and L.P. Pitaevskii, 1987 *Physical kinetics*, Pergamon Press, U.K.

19. K. Tuchin, J. Phys. G: Nucl. Part. Phys. **39** (2012) 025010.
20. S. Li, H-U Yee, *Shear Viscosity of Quark-Gluon Plasma in Weak Magnetic Field in Perturbative QCD: Leading Log* Phys. Rev. **D 97**, 056024 (2018).
21. P. Mohanty, A. Dash, V. Roy, Eur. Phys. J. **A 55** (2019) 35.
22. S. Ghosh, B. Chatterjee, P. Mohanty, A. Mukharjee, H. Mishra, Phys. Rev. **D 100** (2019) 034024. arXiv:1804.00812 [hep-ph].
23. S. Nam and C-W Kao, Phys. Rev. **D 87**, 114003 (2013).
24. A. N. Tawfik, A. M. Diab, and M. T. Hussein, Int. J. Adv. Res. Phys. Sci. **3**, 4 (2016).
25. J. Dey, S. Satapathy, A. Mishra, S. Paul, S. Ghosh, *From Non-interacting to Interacting Picture of Quark Gluon Plasma in presence of magnetic field and its fluid property*, arXiv:1908.04335 [hep-ph].
26. A. Dash, S. Samanta, J. Dey, U. Gangopadhyaya, S. Ghosh, V. Roy, *Anisotropic transport properties of Hadron Resonance Gas in magnetic field*, arxiv: 2002.08781 [nucl-th]
27. A. Das, H. Mishra, R. K. Mohapatra, *Transport coefficients of hot and dense hadron gas in a magnetic field: a relaxation time approach* Phys. Rev. **D 100** (2019) 114004.
28. G. S. Denicol, X. G. Huang, E. Molnár, G. M. Monteiro, H. Niemi, J. Noronha, D. H. Rischke, and Q. Wang, *Nonresistive dissipative magnetohydrodynamics from the Boltzmann equation in the 14-moment approximation*, Phys. Rev. **D 98**, 076009 (2018).
29. Z. Chen, C. Greiner, A. Huang, Z. Xu, *Calculation of anisotropic transport coefficients for an ultrarelativistic Boltzmann gas in a magnetic field within a kinetic approach*, Phys. Rev. **D 101** (2020) 056020.
30. A. Harutyunyan and A. Sedrakian, Phys. Rev. **C 94**, no. 2, 025805 (2016) doi:10.1103/PhysRevC.94.025805 [arXiv:1605.07612 [astro-ph.HE]].
31. B. O. Kerbikov and M. A. Andreichikov, Phys. Rev. **D 91**, no. 7, 074010 (2015) doi:10.1103/PhysRevD.91.074010 [arXiv:1410.3413 [hep-ph]].
32. S. i. Nam, Phys. Rev. **D 86**, 033014 (2012) doi:10.1103/PhysRevD.86.033014 [arXiv:1207.3172 [hep-ph]].
33. K. Hattori, S. Li, D. Satow and H. U. Yee, Phys. Rev. **D 95**, no. 7, 076008 (2017) doi:10.1103/PhysRevD.95.076008 [arXiv:1610.06839 [hep-ph]].
34. M. Kurian, S. Mitra, S. Ghosh, V. Chandra, *Transport coefficients of hot magnetized QCD matter beyond the lowest Landau level approximation* Eur. Phys. J. **C 79** (2019) 134.
35. M. Kurian, V. Chandra, *Effective description of hot QCD medium in strong magnetic field and longitudinal conductivity* Phys. Rev. **D 96** (2017) 114026.
36. B. Feng, *Electric conductivity and Hall conductivity of the QGP in a magnetic field* Phys. Rev. **D 96**, 036009 (2017).
37. K. Fukushima, Y. Hidaka, *Electric conductivity of hot and dense quark matter in a magnetic field with Landau level resummation via kinetic equations* Phys. Rev. Lett. **120**, 162301 (2018).
38. A. Das, H. Mishra, R. K. Mohapatra, *Electrical conductivity and Hall conductivity of a hot and dense hadron gas in a magnetic field: A relaxation time approach* Phys.Rev. **D 99** (2019) 094031.
39. A. Das, H. Mishra, R. K. Mohapatra *Electrical conductivity and Hall conductivity of hot and dense quark gluon plasma in a magnetic field: a quasi particle approach* arXiv:1907.05298 [hep-ph].
40. S. Ghosh, A. Bandyopadhyay, R. L. S. Farias, J. Dey, G. Krein, *Anisotropic electrical conductivity of magnetized hot quark matter*, arXiv:1911.10005.
41. L. Thakur, P.K. Srivastava, *Electrical conductivity of a hot and dense QGP medium in a magnetic field* Phys. Rev. **D 100** (2019) 076016.
42. B. Chatterjee, R. Rath, G. Sarwar, R. Sahoo, *Centrality dependence of Electrical and Hall conductivity at RHIC and LHC energies for a Quark-Gluon Plasma Phase* arXiv: 1908.01121 [hep-ph].
43. M. Kurian, *Thermal transport in a weakly magnetized hot QCD medium*, arXiv:2005.04247 [nucl-th].
44. K. Hattori, X. G. Huang, D. H. Rischke and D. Satow, *Bulk Viscosity of Quark-Gluon Plasma in Strong Magnetic Fields* arXiv:1708.00515 [hep-ph].
45. X-G Huang, M. Huang, D. H. Rischke, A. Sedrakian, *Anisotropic hydrodynamics, bulk viscosities, and r-modes of strange quark stars with strong magnetic fields* Phys. Rev. **D 81**, 045015 (2010).
46. N.O. Agasian, Phys. Atom. Nucl. **76** (2013) 1382.
47. N.O. Agasian, JETP Lett. **95** (2012) 171.
48. M. Kurian, V. Chandra, *Bulk viscosity of a hot QCD medium in a strong magnetic field within the relaxation-time approximation* Phys. Rev. **D 97** (2018) 116008.
49. M. Kurian, S. K. Das, V. Chandra *Heavy quark dynamics in a hot magnetized QCD medium* arXiv:1907.09556 [nucl-th].
50. B. Singh, L. Thakur, H. Mishra *Heavy quark complex potential in a strongly magnetized hot QGP medium* Phys. Rev. **D 97** (2018) 096011.
51. R. Critelli, S.I. Finazzo, M. Zaniboni, J. Noronha, *Anisotropic shear viscosity of a strongly coupled non-Abelian plasma from magnetic branes* Phys. Rev. **D 90** (2014) 066006.
52. S.I. Finazzo, R. Critelli, R. Rougemont, J. Noronha, *Momentum transport in strongly coupled anisotropic plasmas in the presence of strong magnetic fields* Phys.Rev. **D 94** (2016) 054020.
53. K. A. Mamo, JHEP **1308**, 083 (2013).
54. S. Jeon, *Hydrodynamic transport coefficients in relativistic scalar field theory* Phys. Rev. **D 52** (1995) 3591.
55. D. Fernandez-Fraile, A.G. Nicola, *Transport coefficients and resonances for a meson gas in Chiral Perturbation Theory* Eur. Phys. J. **C 62** (2009) 37.
56. S. Ghosh, Int. J. Mod. Phys. **A 29** (2014) 1450054.
57. P. Chakraborty and J. I. Kapusta, Phys. Rev. **C 83**, 014906 (2011).
58. S. Gavin, *Transport Coefficients In Ultrarelativistic Heavy Ion Collisions*, Nucl. Phys. **A 435**, 826 (1985).
59. P. Kovtun, D.T. Son, A.O. Starinets, Phys. Rev. Lett. **94** (2005) 111601.
60. T. Schafer, D. Teaney, *Nearly perfect fluidity: from cold atomic gases to hot quark gluon plasmas* Rep. Prog. Phys. **72** (2009) 126001.
61. X.G. Huang, M. Huang, D. H. Rischke, *Anisotropic Hydrodynamics, Bulk Viscosities and R-Modes of Strange Quark Stars with Strong Magnetic Fields*, Phys. Rev. **D 81** (2010) 045015.
62. X.G. Huang, A. Sedrakian, D. H. Rischke, *Kubo formulas for relativistic fluids in strong magnetic fields*. Annals Phys. **326** (2011) 3075.
63. A. Bandyopadhyay, R.L.S. Farias, *Inverse magnetic catalysis – how much do we know about?* arXiv: 2003.11054 [hep-ph].

64. R.L.S. Farias, K.P. Gomes, G.I. Krein, M.B. Pinto, *Importance of asymptotic freedom for the pseudocritical temperature in magnetized quark matter*, Phys. Rev. **C 90** (2014) 025203.
65. R.L.S. Farias, V.S. Timoteo, S.S. Avancini, M.B. Pinto, G. Krein, *Thermo-magnetic effects in quark matter: Nambu–Jona-Lasinio model constrained by lattice QCD*, Eur. Phys. J. **A 53** (2017) 101.